Electronic Research Archive

https://www.aimspress.com/journal/era

ERA, 34(5): 2805–2838.
DOI: 10.3934/era.2026128
Received: 06 February 2026
Revised: 26 February 2026
Accepted: 04 March 2026
Published: 30 March 2026

Research article

Stochastic stabilization and reliability analysis of discrete-time inertial reaction-diffusion neural networks with delays: Application to robotic manipulators

Yongyan Yang[1], **Tianwei Zhang**[2,*] **and Yuntao Liu**[3]

[1] Department of Mathematics, Puyang Petrochemical Vocational and Technical College, Puyang 457001, China

[2] School of Mathematics and Statistics, Yunnan University, Kunming 650500, China

[3] Oxbridge College, Kunming University of Science and Technology, Kunming 650106, China

* **Correspondence:** Email: zhang@ynu.edu.cn.

Abstract: Discrete-time modeling and reliable control of mechanical systems with inertia, spatial coupling, time delays, and random disturbances are of fundamental importance in mechanism and machine science, particularly for safety-critical and robotic applications. This paper investigated the nonlinear dynamics and stabilization of a class of discrete-time inertial reaction–diffusion mechanical systems subject to stochastic perturbations and time-varying delays. A strong spatio-temporal discretization framework was employed to formulate the system as second-order difference equations incorporating inertial effects, diffusive coupling, delayed interactions, and stochastic excitations. To describe long-term dynamic behavior in noisy environments, a mean-square pseudo almost periodic solution concept was introduced. Sufficient conditions were established to ensure the existence and uniqueness of such solutions via fixed-point techniques. Moreover, a feedback control strategy was developed to achieve global exponential stabilization in the mean-square sense. Explicit stability criteria were derived, revealing the effects of inertia, diffusion intensity, delay bounds, stochastic disturbance levels, and control gains on system reliability and convergence performance. Numerical simulations on a multi-joint robotic manipulator validated the theoretical results and illustrated the trade-off between convergence speed and robustness under stochastic disturbances.

Keywords: neural networks; multibody dynamics; nonlinear dynamics; stochastic effects; control and reliability; robotics application

1. Introduction

Modern safety-critical systems—such as nuclear power plants, chemical processing units, transportation infrastructures, and robotic manipulators—operate under complex, uncertain, and dynamically changing conditions. Ensuring their reliability and safety requires mathematical frameworks that can explicitly capture stochastic disturbances, time delays, and coupling effects that may trigger performance degradation or failure propagation. Reliability engineering traditionally relies on probabilistic and statistical models to estimate failure probabilities and hazard rates; however, these models often lack the ability to represent the high-dimensional nonlinear dynamics underlying system interactions. Inertial neural networks (INNs) (see [1, 2]) are an emerging class of recurrent neural network (RNN) architectures [3, 4] inspired by the principles of dynamical systems, particularly mechanical systems [3] characterized by inertia, damping, and friction. By providing a rigorous mathematical framework for such dynamics, INNs can serve as a foundation for reliability-enhancing strategies, ranging from early warning mechanisms to adaptive control protocols that ensure stable and safe operation [5] under uncertain and varying conditions (see [6–9]).

Discrete reaction–diffusion equations, especially when extended to incorporate stochastic perturbations [10], offer a powerful mathematical tool for representing spatiotemporal interactions within these systems [11–13]. Their discrete-space formulations enable detailed modeling of localized interactions and long-range coupling in networked environments, which is particularly valuable in reliability engineering for understanding how failures, disturbances, or hazardous events propagate across interconnected subsystems. In scenarios such as distributed sensor networks for structural health monitoring, automated fault detection in manufacturing plants, or dynamic hazard assessment in transportation infrastructures, these equations capture both the immediate impact of local faults and their potential to escalate into system-wide failures. The inclusion of stochastic effects—arising from measurement noise, environmental variability, or inherent system uncertainties—makes it possible to conduct probabilistic safety assessments and evaluate the robustness of operational strategies. By embedding these stochastic reaction–diffusion dynamics [14] within inertial neural network models, one can investigate the interplay between local and global stability properties, identify vulnerabilities to cascading effects, and design control strategies that not only stabilize the system but also improve resilience against rare, high-impact events.

Stochastic difference equations (SDEs) form a powerful mathematical framework [6] for characterizing dynamic processes in which deterministic evolution is influenced by random perturbations. In the domain of reliability engineering, such tools are indispensable for representing and analyzing the impact of uncertainty on complex technological systems [15]. Sources of uncertainty may include measurement noise in sensor networks, variability in operational loads, component wear and degradation, and environmental hazards such as fluctuating temperatures, wind, or seismic activity [12, 13]. Modeling these factors within a discrete space–time structure enables engineers to track how disturbances originating at a local scale can propagate across interconnected subsystems, potentially compromising global system performance or safety. This perspective is critical for probabilistic safety assessment and dynamic reliability analysis in applications such as nuclear power plant control under fluctuating coolant flow rates, chemical process plants subject to stochastic feedstock variations, transportation networks exposed to

random traffic surges, or offshore oil platforms operating in highly variable marine environments [16–18]. Despite the rapid progress in stochastic system theory and intelligent control, the integration of rigorous mathematical stability results with reliability-oriented decision-making remains limited. Existing studies primarily focus on deterministic stability or performance optimization, often neglecting how stochastic disturbances, delayed feedback, and spatial interactions affect system reliability, failure propagation, and safety margins. To address this gap, the present work develops a probabilistic framework that connects stochastic difference equations, reaction–diffusion dynamics, and INNs under discrete space–time settings.

Motivated by the need for reliability-oriented control and decision tools, this work proposes a discrete-space-time SINN framework incorporating stochastic perturbations and delays [19]. The new concept of MS-(μ, ν)-PWAPS captures quasi-periodic behavior in the mean-square sense, allowing long-term reliability prediction under random influences. The theoretical results yield explicit conditions that guarantee bounded failure probability, robust stabilization, and reliability enhancement in networked engineering systems. Almost periodic sequences (APSs) (see [20–22]) and their generalizations, such as Weyl almost periodic sequences (WAPSs), provide a rigorous mathematical framework for describing recurrent yet non-exact patterns in system behavior. Embedding WAPS analysis into stochastic INNs makes it possible to detect, classify, and predict these patterns over long time horizons, even in the presence of nonlinear interactions and environmental disturbances. For safety-critical systems, such as transportation infrastructure or offshore platforms, this approach enables early identification of abnormal trends, assessment of resilience against recurring stressors, and formulation of proactive control measures that maintain the system within safe operational envelopes. By integrating the theoretical strengths of almost periodicity with probabilistic modeling, engineers can bridge the gap between abstract dynamical analysis and actionable safety management in complex, uncertainty-prone environments [23–25].

In dynamical systems theory, stability [5, 26] is a cornerstone concept that characterizes how a system responds to internal or external disturbances, determining whether its behavior will converge toward a safe operating state or drift toward unsafe and potentially catastrophic conditions [27–29]. Within the field of reliability engineering, this concept is central to ensuring that complex technological systems—ranging from nuclear power plants and chemical processing units to aerospace vehicles, maritime platforms, and intelligent transportation networks—maintain predictable, bounded, and controllable behavior under a wide range of operational scenarios. In these safety-critical domains, loss of stability can manifest as uncontrolled oscillations, cascading subsystem failures, or rapid performance degradation, each of which may lead to severe safety hazards and operational downtime. Lyapunov stability theory provides a mathematically rigorous and widely applicable framework for quantifying such behaviors. By constructing suitable Lyapunov functions, engineers and researchers can derive precise conditions under which disturbances—whether from environmental events like earthquakes and wind gusts, from component degradation, or from human operational errors—decay over time rather than amplify. This methodology supports the formulation of robust control laws that actively suppress unsafe transients, mitigate oscillatory responses, and ensure recovery to nominal operating states. In practical engineering applications, these stability guarantees are essential for designing control systems that meet stringent safety criteria, comply with regulatory standards, and remain effective in the presence of parameter uncertainties or unpredictable disturbances. The challenge becomes even greater in high-dimensional, nonlinear, and stochastic architectures such as stochastic inertial neural networks (SINNs), where complex coupling effects, spatial

diffusion, time delays, and stochastic perturbations interact in nontrivial ways. In such systems, traditional stability analysis [30] may be insufficient, necessitating new theoretical tools and stabilization strategies [31–35] that can handle the intricate blend of deterministic dynamics and probabilistic variability. By extending stability theory to accommodate these features, the research not only advances the mathematical understanding of complex dynamical networks [36] but also provides actionable methods for enhancing safety, reliability, and fault tolerance in engineered systems [37] that operate under uncertainty and are subject to real-world operational constraints.

Building on the preceding discussion, this paper pursues two tightly connected objectives in safety-critical engineered systems. First, we introduce and rigorously characterize mean-square (μ, ν)-pseudo Weyl almost periodic sequences (MS-(μ, ν)-PWAPSs) for discrete stochastic inertial neural networks (SINNs), establishing conditions for existence, uniqueness, and long-term stability in the presence of stochastic disturbances, spatial diffusion, and delays. Second, we develop and analyze feedback control strategies that guarantee global exponential stabilization of SINNs under Euler–Maruyama noise and time delays, and we elucidate the engineering trade-offs between control gains and convergence rates. These contributions are motivated by and linked to reliability challenges in complex technological systems, where methods that support probabilistic safety assessment and dynamic reliability are essential for maintaining predictable and safe operation under uncertainty. Numerical simulations on robotic joint dynamics substantiate the theory and yield actionable design guidelines for parameter tuning (diffusion, damping, and control coefficients) that balance rapid convergence with stability margins, thereby bridging advanced stochastic analysis with practical reliability engineering needs.

1) This paper introduces the novel concept of MS-(μ, ν)-PWAPSs to model the dynamic behavior of SINNs in discrete space-time, thereby extending conventional discrete-time RNN models [3, 4] to incorporate both spatial and temporal discretization. By extending traditional almost periodicity and Weyl almost periodicity frameworks [13, 20–25], this approach advances the theoretical tools for analyzing the reliability and stability of complex stochastic systems subject to random disturbances. The proposed framework supports the assessment and control of system performance in uncertain environments, contributing to the development of robust methods for enhancing the safety and reliability of intelligent networked systems. These contributions align with recent advances in reliability engineering, such as the use of physics-guided neural networks for structural prognostics [3] and the application of Lyapunov-stability methods for critical infrastructure protection [4].

2) For the first time, this study investigates Weyl almost periodicity and pseudo-almost periodicity in SINNs within a discrete space-time framework, addressing a critical gap in the existing literature on (Weyl) almost periodic sequences [13,21,23,24]. By incorporating SDEs and Euler–Maruyama noise, the work rigorously analyzes the influence of random disturbances on neural network dynamics. This research contributes to the development of robust mathematical models and analytical techniques for assessing and enhancing the reliability and stability of complex intelligent systems operating under uncertainty. The stochastic modeling approach complements recent studies on safety exploration for uncertain systems [15] and degrading systems [10].

3) We have proposed rigorous theoretical conditions for global exponential stabilization of stochastic inertial neural networks subject to noise and time-delay disturbances, utilizing feedback control strategies to ensure robust system stability. We demonstrated the existence and global exponential stability of a unique MS-(μ, ν)-PWAPS under well-defined conditions. This work advances methods for enhancing the reliability and resilience of complex dynamic systems operating in uncertain environments, directly contributing to probabilistic safety assessment and dynamic reliability analysis. The control framework extends recent innovations for Lyapunov stability [4] and process control [31].

4) Comprehensive numerical simulations on robotic joint dynamics validate the theoretical results and reveal how variations in diffusion coefficients, damping, and control parameters influence convergence and robustness. The outcomes highlight critical engineering trade-offs: while appropriate control tuning accelerates convergence and enhances stability, excessive control can induce instability. These insights offer practical design guidelines for balancing control intensity and stability, thereby contributing to the development of reliability-oriented, fault-tolerant control strategies applicable to safety-critical systems operating under uncertainty.

Collectively, these contributions establish a unified framework that embeds probabilistic reliability concepts into stochastic neural-network-based control theory. The approach enhances the capability to predict, quantify, and manage reliability risks in complex dynamic systems operating under uncertainty.

Symbols: $\mathbb{R}^n$ denotes the space of n-dimensional real vectors and $\|\cdot\|$ is the norm of $\mathbb{R}^n$; $\mathbb{Z}$ is the set of integral numbers; $\mathbb{Z}_0 = \{0, 1, 2, \ldots\}$; $\mathbb{Z}_+ = \mathbb{Z}_0 \backslash \{0\}$; $I_J = I \cap J$, $\forall I, J \subseteq \mathbb{R}$. For any function $z = z_k^{[\iota]} : \mathbb{Z} \times \mathbb{Z} \to \mathbb{R}$, denote $\Delta z_k^{[\iota]} = z_{k+1}^{[\iota]} - z_k^{[\iota]}$, $\Delta^2 z_k^{[\iota]} = z_{k+2}^{[\iota]} - 2z_{k+1}^{[\iota]} + z_k^{[\iota]}$, $\Delta_\iota^2 z_k^{[\iota]} = \frac{z_k^{[\iota+1]} - 2z_k^{[\iota]} + z_k^{[\iota-1]}}{\hbar^2}$, where $(\iota, k) \in \mathbb{Z} \times \mathbb{Z}$, $\hbar > 0$.

2. System model and mathematical preliminaries

This section develops the theoretical framework for spatiotemporal discrete SINNs. A time-delayed discrete model is derived via the Euler-Maruyama method, along with its recursive solution. We define APSs, WAPSs, and their stochastic extensions, introducing probability spaces and random shift operations. Mathematical tools (e.g., the Minkowski inequality) are presented to support later analysis.

In accordance with the Euler-Maruyama method [38], the present article examines the following space-time discrete SINNs involving time delays:

$$\begin{cases} \Delta^2 z_{i,k}^{[\iota]} = 2(e^{-\frac{1}{2}a_i h} - 1)\Delta z_{i,k}^{[\iota]} + \left[\dfrac{2 - 2e^{-\frac{1}{2}a_i h}}{a_i}\right]^2 \Big[\gamma_i \Delta_\iota^2 z_{i,k}^{[\iota]} - b_{i,k} z_{i,k}^{[\iota]} \\ \qquad\qquad + \displaystyle\sum_{j=1}^{n} c_{ij,k} f_j(z_{j,k-\delta_{j,k}}^{[\iota]}) + \frac{1}{\sqrt{h}} \sum_{j=1}^{n} \xi_{ij,k} \sum_{l=1}^{\infty} \sigma_{jl}(z_{j,k-o_{j,k}}^{[\iota]}) \varepsilon_{l,k} + I_{i,k} \Big], \quad \forall \iota \in (0, \aleph)_{\mathbb{Z}}, \\ z_{i,k}^{[\iota]}\Big|_{\iota \in \{0,\aleph\}} = 0, \quad \forall k \in \mathbb{Z}, i = 1, 2, \ldots, n, \end{cases} \tag{2.1}$$

where z_i shows the ith neuron; a_i represents the damping, while $b_i > 0$ indicates the strength of the i-th neuron; γ_{ip} corresponds to the diffusion; c_{ij} and μ_{ij} denote the synaptic coupling strengths; f_j represents the activation function, while σ_{jl} corresponds to the noise function; ξ_{ij} stands for the noise intensity; I_i signifies the external input; $\hbar$ and h indicate the respective lengths of the space and time steps; $\varepsilon_{l,k} = \frac{B_l(kh+h) - B_l(kh)}{\sqrt{h}} \sim$

$\mathcal{N}(0,1)$ stands for the normal distribution with mean 0 and covariance 1, and $\{B_l\}_{l\in\mathbb{Z}_+}$ consists of scalar-valued, mutually independent, two-sided standard Brownian motions defined on the canonical Wiener space $(\Theta, \mathscr{F}, \mathbb{P})$.

Remark 2.1. *As described in [12, 13], SINN* (2.1) *is derived from a full discretization of continuous INNs governed by reaction-diffusion systems, featuring strong spatiotemporal discretization where both time and space variables are rigorously discretized. Unlike previous works [3, 4] that only considered temporal discretization of neural networks, our approach employs: 1) the exponential Euler method for time discretization, 2) central finite differences for spatial discretization, and 3) the Euler-Maruyama method for the Brownian motions. This complete spatiotemporal framework enables precise modeling of both localized interactions and long-range coupling effects in networked systems, which is particularly crucial for reliability analysis in safety-critical applications [4, 5]. The spatial discretization scheme maintains convergence properties while capturing essential diffusion phenomena that are completely absent in pure temporal-discretization models like those in [3, 4]. For implementation details of this comprehensive discretization approach, see [12, 13].*

Further, the definition of mean-squared ergodic Weyl ϑ-almost periodic sequences was outlined in the literature [39] and is included below. In order to introduce the concept of the Weyl almost periodic sequence, it is necessary to define the norm and space below

$$\|z\|_{\mathbb{W}^2} = \lim_{K\to+\infty}\sup_{k\in\mathbb{Z}}\left[\frac{1}{K}\sum_{s=k}^{k+K-1}\|z_s\|_{\mathbb{X}}^2\right]^{\frac{1}{2}}, \quad \forall z:\mathbb{Z}\to\mathbb{X}, \quad \mathbb{BW}^2(\mathbb{Z},\mathbb{X}) = \Big\{z:\mathbb{Z}\to\mathbb{X}\Big|\|z\|_{\mathbb{W}^2}<\infty\Big\}.$$

Hereby, $(\mathbb{X}, \|\cdot\|_{\mathbb{X}})$ denotes some Banach space. Define $\mathscr{M}$ as the collection of all measures on some σ-field of $\mathbb{Z}$, which also meet $\mu(\mathbb{Z}) = \infty$ and $\varkappa_0(b-a) \le \mu([a,b]_{\mathbb{Z}}) < \varkappa_1(b-a)$ for each $\mu \in \mathscr{M}$. For all $a, b(a<b) \in \mathbb{Z}$, $\varkappa_0, \varkappa_1$ are two constants. Throughout this article, let μ, ν belong to $\mathscr{M}$.

Definition 2.1. ([40]) *A real bounded sequence* $\{z_k\}_{k\in\mathbb{Z}} : \mathbb{Z}\to\mathbb{X}$ *is* (μ,ν)***-ergodic*** *in the case where* $\lim_{\ell\to+\infty}\frac{1}{\nu([-\ell,\ell]_{\mathbb{Z}})}\sum_{s=-\ell}^{\ell-1}\|z_s\|_{\mathbb{X}}\mu([s,s+1]_{\mathbb{Z}}) = 0$. *All of such sequences are denoted by* $\mathbb{ERG}(\mathbb{Z},\mathbb{X},\mu,\nu)$.

In order to identify the solution process in question, it is necessary to establish a suitable probabilistic setting in which a random dynamical system (see [39]) can be defined. As outlined in [39, Proposition 1.4.4], we introduce the canonical (two-sided) Wiener space $(\Theta, \mathscr{F}, \mathbb{P})$ satisfying: **a)** $\Theta = C_0(\mathbb{R}, S)$, where S denotes the space of all real number sequences and $C_0(\mathbb{R}, S)$ is the space of all continuous functions $\omega : \mathbb{R}\to S$ with $\omega(0) = 0 \in S$. **b)** $\mathscr{F}$ represents the Borel σ-algebra on Θ. **c)** The Wiener measure $\mathbb{P}$ on $(\Theta, \mathscr{F})$ makes the processes $B_1(t,\omega), B_2(t,\omega), \ldots$ defined by $(B_1(t,\omega), B_2(t,\omega), \ldots)^T := \omega(t) = (\omega_1(t), \omega_2(t), \ldots)^T$ for $\omega \in \Theta$ be independent one-dimensional Brownian motions. **d)** The sub-σ-algebra $\mathscr{F}_s^t$ is the σ-algebra generated by $\omega(u) - \omega(v)$ for $s \le v \le u \le t$. **e)** The family of shifts $(\vartheta_t)_{t\in\mathbb{R}}$ on $(\Theta, \mathscr{F}, \mathbb{P})$, given by $\vartheta_t\omega(\cdot) := \omega(t+\cdot) - \omega(t)$, is measure-preserving and ergodic.

For any $t, \tau \in \mathbb{R}$ and $\omega \in \Theta$, it holds that $B_l(t+\tau, \vartheta_{-\tau}\omega) = B_l(t,\omega) - B_l(-\tau,\omega), l = 1, 2, \ldots$. Let $\mathbb{E}$ be the expectation on $(\Theta, \mathscr{F}, \mathbb{P})$ and

$$\mathbb{L}^2(\mathbb{P},\mathbb{R}^n) = \left\{z = (z_1,\ldots,z_n)^T : \Theta\to\mathbb{R}^n \middle| \|z_i\|_2 := \Big[\mathbb{E}|z_i|^2\Big]^{1/2} < \infty, 1 \le i \le n\right\}.$$

Define a shift operation of the random process $z_k \in \mathbb{L}^2(\mathbb{P},\mathbb{R})$ by $\mathfrak{T}_s z_k(\omega) := z_{k+s}(\vartheta_{-s}\omega), \forall k, s \in \mathbb{Z}, \omega \in \Theta$. We can easily deduce that $\mathfrak{T}_\tau\Big[B_l(t+s,\omega) - B_l(t,\omega)\Big] = B_l(t+s,\omega) - B_l(t,\omega), \forall t, s \in \mathbb{R}, \tau \in \mathbb{Z}, \omega \in \Theta, l = 1, 2, \ldots$.

Definition 2.2. ([41, Definition 3.2]) *Let $z_k \in \mathbb{L}^2(\mathbb{P},\mathbb{R}^n)$ for any $k \in \mathbb{Z}$. Assume that $\left\{\tau \in \mathbb{Z}\middle| \|\mathfrak{T}_\tau z_k - z_k\|_2 < \epsilon, \forall k \in \mathbb{Z}\right\}$ is relatively dense in $\mathbb{Z}$ for each $\epsilon > 0$, and then z is said to be a mean squared ϑ-almost periodic sequence. Hereby, τ is called the ϵ-almost period. All ϑ-almost periodic sequences are expressed by $\mathbb{AP}^\vartheta(\mathbb{Z},\mathbb{L}^2(\mathbb{P},\mathbb{R}^n))$.*

Definition 2.3. ([42]) *Assume that $z \in \mathbb{BW}^2(\mathbb{Z},\mathbb{L}^2(\mathbb{P},\mathbb{R}^n))$ and $f : \mathbb{Z}\times\mathbb{BW}^2(\mathbb{Z},\mathbb{L}^2(\mathbb{P},\mathbb{R}^n)) \to \mathbb{R}^n$, and then we say that the sequence $\{z_k\}_{k\in\mathbb{Z}}$ is mean-squared Weyl ϑ-almost periodic if*

$$\left\{\tau \in \mathbb{Z}\middle| \|\mathfrak{T}_\tau z - z\|_{\mathbb{W}^2} = \lim_{K\to+\infty}\sup_{k\in\mathbb{Z}}\left[\frac{1}{K}\sum_{s=k}^{k+K-1}\|\mathfrak{T}_\tau z_s - z_s\|_2^2\right]^{\frac{1}{2}} < \epsilon\right\}$$

is relatively dense in $\mathbb{Z}$ for each $\epsilon > 0$. Hereby, τ is called the ϵ-Weyl almost period. All such functions are denoted by $\mathbb{W}^2\mathbb{AP}^\vartheta(\mathbb{Z},\mathbb{L}^2(\mathbb{P},\mathbb{R}^n))$.

Definition 2.4. ([25]) *A stochastic sequence $z \in \mathbb{BW}^2(\mathbb{Z},\mathbb{L}^2(\mathbb{P},\mathbb{R}^n))$ is called mean-squared (μ,ν)-pseudo Weyl ϑ-almost periodic in the case where $z = z_1 + z_2$, where $z_1 \in \mathbb{W}^2\mathbb{AP}^\vartheta(\mathbb{Z},\mathbb{L}^2(\mathbb{P},\mathbb{R}^n))$ and $z_2 \in \mathbb{ERG}(\mathbb{Z},\mathbb{L}^2(\mathbb{P},\mathbb{R}^n),\mu,\nu)$ (see* Definition 2.1*). All such sequences are denoted by $\mathbb{W}^2\mathbb{PAP}^\vartheta(\mathbb{Z},\mathbb{L}^2(\mathbb{P},\mathbb{R}^n),\mu,\nu)$.*

Lemma 2.1. ([6]) *If $a > 0$, then $\sum_{q=k_0}^{k-1}\sum_{\zeta=k_0}^{q-1} e^{-a(k-\zeta-2)h} \le (1-e^{-ah})^{-2}, \forall k \ge k_0, k, k_0 \in \mathbb{Z}$.*

Lemma 2.2. *Let $a > 0$, $u : \mathbb{Z}\times[0,\aleph]_\mathbb{Z} \to \mathbb{L}^2(\mathbb{P},\mathbb{R}^n)$, and $\|u_k^{[\iota]}\|_2 = \sqrt{\mathbb{E}\|u_k^{[\iota]}\|^2} < \infty$, $\forall(k,\iota) \in \mathbb{Z}\times[0,\aleph]_\mathbb{Z}$. Then*

1) for any $(k,q) \in (q_1,+\infty)_\mathbb{Z}\times(\zeta_1,+\infty)_\mathbb{Z}$, $\mathbb{E}[\sum_{q=q_1}^{k-1}\sum_{\zeta=\zeta_1}^{q-1} e^{-a(k-\zeta-2)h}u_\zeta^{[\cdot]}]^2 \le \frac{1}{(1-e^{-ah})^4}\sup_{k\in\mathbb{Z}}\|u_k^{[\cdot]}\|_2^2$, where $q_1,\zeta_1 \in \mathbb{Z}\cup\{-\infty\}$.

2) for any $q_*,\zeta_* \in \mathbb{Z}$, $q_* \ge \zeta_*$ and $k \in [q_*,+\infty)_\mathbb{Z}$, $\mathbb{E}[\sum_{q=q_*}^{k-1}\sum_{\zeta=\zeta_*}^{q-1} e^{-a(k-\zeta-2)h}u_{\zeta-\delta_\zeta}^{[\cdot]}]^2 \le \frac{2(1+\delta_\infty)e^{ah\delta_\infty}}{\epsilon h(1-e^{-ah})^2}\sum_{\zeta=\zeta_*-\delta_\infty}^{k-1} e^{-a_\epsilon(k-\zeta-2)h}\|u_\zeta^{[\cdot]}\|_2^2$, where $0 \le \delta_k \le \delta_\infty$ for all $k \in \mathbb{Z}$, $a_\epsilon := a-\epsilon$, and $0 < \epsilon < \min\{a, \frac{1}{h}\}$.

Proof. By utilizing Hölder inequalities twice, we attain

$$\begin{aligned}\mathbb{E}\Big[\sum_{q=q_1}^{k-1}\sum_{\zeta=\zeta_1}^{q-1} e^{-a(k-\zeta-2)h}u_\zeta^{[\cdot]}\Big]^2 &\le \frac{1}{1-e^{-ah}}\sum_{q=q_1}^{k-1} e^{-a(k-q-1)h}\Big[\sum_{\zeta=\zeta_1}^{q-1} e^{-a(q-\zeta-1)h}\cdot\sum_{\zeta=\zeta_1}^{q-1} e^{-a(q-\zeta-1)h}\mathbb{E}\|u_\zeta^{[\cdot]}\|^2\Big]\\ &\le \frac{1}{(1-e^{-ah})^4}\sup_{k\in\mathbb{Z}}\|u_k^{[\cdot]}\|_2^2.\end{aligned}$$

So 1) is satisfied.

Similarly, for any $q_*,\zeta_* \in \mathbb{Z}$, $q_* \ge \zeta_*$ and $k \in [q_*,+\infty)_\mathbb{Z}$, 2) holds based on the fact that

$$\begin{aligned}\mathbb{E}\Big[\sum_{q=q_*}^{k-1}\sum_{\zeta=\zeta_*}^{q-1} e^{-a(k-\zeta-2)h}u_{\zeta-\delta_\zeta}^{[\cdot]}\Big]^2 &\le \frac{1}{(1-e^{-ah})^2}\sum_{q=q_*}^{k-1}\sum_{\zeta=\zeta_*}^{q-1} e^{-a(k-\zeta-2)h}\mathbb{E}\|u_{\zeta-\delta_\zeta}^{[\cdot]}\|^2\\ &= \frac{1}{(1-e^{-ah})^2}\sum_{\zeta=\zeta_*}^{k-2} e^{-a(k-\zeta-2)h}(k-\zeta-1)\mathbb{E}\|u_{\zeta-\delta_\zeta}^{[\cdot]}\|^2\end{aligned}$$

$$\begin{aligned}
&\leq \frac{2}{\epsilon h(1-e^{-ah})^2}\sum_{\zeta=\zeta_*}^{k-1}\sum_{l=0}^{\delta_\infty} e^{-a_\epsilon(k-\zeta-2)h}\mathbb{E}\|u_{\zeta-l}^{[\cdot]}\|^2\\
&\overset{\zeta'=\zeta-l}{=\!=} \frac{2}{\epsilon h(1-e^{-ah})^2}\sum_{l=0}^{\delta_\infty}\sum_{\zeta'=\zeta_*-l}^{k-l-1} e^{-a_\epsilon(k-\zeta'-l-2)h}\mathbb{E}\|u_{\zeta'}^{[\cdot]}\|^2\\
&\leq \frac{2(1+\delta_\infty)e^{ah\delta_\infty}}{\epsilon h(1-e^{-ah})^2}\sum_{\zeta'=\zeta_*-\delta_\infty}^{k-1} e^{-a_\epsilon(k-\zeta'-2)h}\|u_{\zeta'}^{[\cdot]}\|_2^2.
\end{aligned}$$

This completes the proof.

Lemma 2.3. ([43, Theorem 1.6]) *Supposing $\{z_k\}_{k=0}^{\infty}$ is a non-negative sequence, $\{g_k\}_{k=0}^{\infty}$ is a non-negative and non-decreasing sequence, and $z_k \leq a\sum_{q=0}^{k-1} z_q + g_k, \forall k \in \mathbb{Z}_0$, then $z_k \leq g_k e^{ak}, \forall k \in \mathbb{Z}_0$.*

Lemma 2.4. ([44] *Assume that $p_k, g_k \in \mathbb{R}$ and $p_{k+1} = \lambda p_k + g_k, \forall k \in \mathbb{Z}_0$. Then $p_k = \lambda^k p_0 + \sum_{q=0}^{k-1}\lambda^{k-q-1}g_q, \forall k \in \mathbb{Z}_0\backslash\{0\}$.*

3. Ergodic Weyl almost periodicity in stochastic neural networks

This section systematically investigates the dynamical properties of mean-square (μ,ν)-pseudo Weyl almost periodic sequences (MS-(μ,ν)-PWAPSs) in SINNs. This research not only provides a novel approach for analyzing the ergodicity and almost periodicity of discrete space-time stochastic systems but also offers significant insights for stability control in high-dimensional nonlinear systems within neuromorphic computing. The findings are particularly applicable to neural network modeling involving inertial effects and noise disturbances. For the remainder of this study, we impose these key assumptions.

(i_1) δ_j and o_j are almost periodic sequences, $j = 1, 2, \ldots, n$.

(i_2) b_i, c_{ij}, ξ_{ij}, and I_i are bounded $\mathbb{R}$-valued (μ,ν)-pseudo Weyl almost periodic sequences, $i, j = 1, 2, \ldots, n$.

(i_3) $f_j(0) = \sigma_{jl}(0) = 0$ and there exist positive numbers L_j^f and L_{jl}^σ such that $|f_j(u) - f_j(v)| \leq L_j^f|u - v|, |\sigma_{jl}(u) - \sigma_{jl}(v)| \leq L_{jl}^\sigma|u - v|, \forall u, v \in \mathbb{R}, j = 1, 2, \ldots, n$.

(i_4) $L_{j*}^\sigma := \sum_{l=1}^{\infty} L_{jl}^\sigma < \infty$, $j = 1, 2, \ldots, n$.

For any $\mathbf{z} \in \mathbb{W}^2\mathbb{PAP}^\vartheta(\mathbb{Z}\times[0,\aleph]_\mathbb{Z}, \mathbb{L}^2(\mathbb{P},\mathbb{R}^n),\mu,\nu)$ with $\mathbf{z} = (z_1, z_2, \ldots, z_n)^T$, define $\Phi : \mathbb{W}^2\mathbb{PAP}^\vartheta(\mathbb{Z}\times[0,\aleph]_\mathbb{Z}, \mathbb{L}^2(\mathbb{P},\mathbb{R}^n),\mu,\nu) \to \mathbb{R}^n$ by $\Phi\mathbf{z} = ((\Phi\mathbf{z})_1, (\Phi\mathbf{z})_2, \ldots, (\Phi\mathbf{z})_n)^T$, where

$$\begin{aligned}
(\Phi\mathbf{z})_{i,k}^{[\iota]} = \alpha_i^2\sum_{q=-\infty}^{k-1}\sum_{\zeta=-\infty}^{q-1} e^{-\frac{1}{2}a_i(k-\zeta-2)h}\Big[&\gamma_i\Delta_\iota^2 z_{i,\zeta}^{[\iota]} + \Big(\frac{1}{4}a_i^2 - b_{i,\zeta}\Big)z_{i,\zeta}^{[\iota]}\\
&+\sum_{j=1}^{n} c_{ij,\zeta}f_j(z_{j,\zeta-\delta_{j,\zeta}}^{[\iota]}) + \frac{1}{\sqrt{h}}\sum_{j=1}^{n}\xi_{ij,\zeta}\sum_{l=1}^{\infty}\sigma_{jl}(z_{j,\zeta-o_{j,\zeta}}^{[\iota]})\varepsilon_{l,\zeta} + I_{i,\zeta}\Big],
\end{aligned} \tag{3.1}$$

where $\alpha_i := \frac{2-2e^{-\frac{1}{2}a_ih}}{a_i}$, $(\iota,k) \in (0,\aleph)_\mathbb{Z}\times\mathbb{Z}$, and $(\Phi\mathbf{z})_{i,k}^{[\iota]}\Big|_{\iota\in\{0,\aleph\}} = 0, \forall k \in \mathbb{Z}, i = 1, 2, \ldots, n$.

3.1. Propositions

For arbitrary $\mathbf{z} \in \mathbb{W}^2\mathbb{PAP}^{\vartheta}(\mathbb{Z} \times [0,\aleph]_{\mathbb{Z}}, \mathbb{L}^2(\mathbb{P},\mathbb{R}^n),\mu,\nu)$, define $\|\mathbf{z}\|_\infty = \sup_{k\in\mathbb{Z}} \|\mathbf{z}_k\|_*, \|\mathbf{z}_k\|_* = \max_{1\le i\le n} \max_{\iota\in[0,\aleph]_{\mathbb{Z}}} \|z_{i,k}^{[\iota]}\|_2$, in which $\|z_{i,k}^{[\iota]}\|_2 = [\mathbb{E}(z_{i,k}^{[\iota]})^2]^{\frac{1}{2}}$ for $(\iota,k) \in [0,\aleph]_{\mathbb{Z}} \times \mathbb{Z}, i = 1,2,\ldots,n$. Define $a_* := \min_{1\le i\le n} a_i$, $\bar{b}_i := \sup_{k\in\mathbb{Z}} \left|\frac{1}{4}a_i^2 - b_{i,k}\right|, \bar{I}_i := \sup_{k\in\mathbb{Z}} |I_{i,k}|, \bar{c}_{ij} := \sup_{k\in\mathbb{Z}} |c_{ij,k}|, \bar{\xi}_{ij} := \sup_{k\in\mathbb{Z}} |\xi_{ij,k}|$, where $i,j = 1,2,\ldots,n$.

The proofs for the results that follow can be found in Appendix A.

Proposition 3.1. *If $z \in \mathbb{ERG}(\mathbb{Z},\mathbb{L}^2(\mathbb{P},\mathbb{R}),\mu,\nu)$ and $0 \le \delta_k \le \delta_\infty$ for all $k \in \mathbb{Z}$, then $z_{k-\delta_k} \in \mathbb{ERG}(\mathbb{Z},\mathbb{L}^2(\mathbb{P},\mathbb{R}),\mu,\nu)$.*

Proposition 3.2. *Let $\delta_k : \mathbb{Z} \to [0,\delta_\infty]_{\mathbb{Z}}$ be an almost periodic sequence, $\forall k \in \mathbb{Z}$. If $z \in \mathbb{W}^2\mathbb{AP}^{\vartheta}(\mathbb{Z},\mathbb{L}^2(\mathbb{P},\mathbb{R}))$, then $z_{k-\delta_k} \in \mathbb{W}^2\mathbb{AP}^{\vartheta}(\mathbb{Z},\mathbb{L}^2(\mathbb{P},\mathbb{R}))$, $\forall k \in \mathbb{Z}$.*

Proposition 3.3. *Let $z \in \mathbb{W}^2\mathbb{PAP}^{\vartheta}(\mathbb{Z},\mathbb{L}^2(\mathbb{P},\mathbb{R}),\mu,\nu)$ and $0 \le \delta_k \le \delta_\infty$ for all $k \in \mathbb{Z}$. So $z_{k-\delta_k} \in \mathbb{W}^2\mathbb{PAP}^{\vartheta}(\mathbb{Z},\mathbb{L}^2(\mathbb{P},\mathbb{R}),\mu,\nu)$.*

Proof. It is a direct conclusion of Propositions 3.1 and 3.2. This completes the proof.

Proposition 3.4. *If $b \in \mathbb{W}^2\mathbb{PAP}(\mathbb{Z},\mathbb{R},\mu,\nu)$ with $|b| \le b_0 < \infty$, $z \in \mathbb{W}^2\mathbb{PAP}^{\vartheta}(\mathbb{Z},\mathbb{L}^2(\mathbb{P},\mathbb{R}),\mu,\nu)$ with $\|z\|_\infty \le z_0 < \infty$, $f(0) = 0$, and $f : \mathbb{R}^n \to \mathbb{R}^n$ with Lipschitz constant $L_f > 0$, then $bf(z) \in \mathbb{W}^2\mathbb{PAP}^{\vartheta}(\mathbb{Z},\mathbb{L}^2(\mathbb{P},\mathbb{R}),\mu,\nu)$.*

Proposition 3.5. *If assumption (i_3) holds and $\mathbf{z} = (z_1,z_2,\ldots,z_n)^T \in \mathbb{W}^2\mathbb{PAP}^{\vartheta}(\mathbb{Z},\mathbb{L}^2(\mathbb{P},\mathbb{R}^n),\mu,\nu)$, then $\sum_{l=1}^{\infty} \sigma_{jl}(z_{j,k})\varepsilon_{l,k} \in \mathbb{W}^2\mathbb{PAP}^{\vartheta}(\mathbb{Z},\mathbb{L}^2(\mathbb{P},\mathbb{R}),\mu,\nu)$, $\forall k \in \mathbb{Z}$.*

Proposition 3.6. *If $a > 0$ and $z = \hat{z} + \check{z} \in \mathbb{W}^2\mathbb{PAP}^{\vartheta}(\mathbb{Z},\mathbb{L}^2(\mathbb{P},\mathbb{R}),\mu,\nu)$ is bounded, then $\hat{\Lambda}_k = \sum_{q=-\infty}^{k-1} \sum_{s=-\infty}^{q-1} e^{-a(k-s-2)h}\hat{z}_s \in \mathbb{W}^2\mathbb{AP}^{\vartheta}(\mathbb{Z},\mathbb{L}^2(\mathbb{P},\mathbb{R}))$, $\forall k \in \mathbb{Z}$, where $\hat{z} \in \mathbb{W}^2\mathbb{AP}^{\vartheta}(\mathbb{Z},\mathbb{L}^2(\mathbb{P},\mathbb{R}))$, $\check{z} \in \mathbb{ERG}(\mathbb{Z},\mathbb{L}^2(\mathbb{P},\mathbb{R}),\mu,\nu)$.*

Proposition 3.7. *If $a > 0$ and $z = \hat{z} + \check{z} \in \mathbb{W}^2\mathbb{PAP}^{\vartheta}(\mathbb{Z},\mathbb{L}^2(\mathbb{P},\mathbb{R}),\mu,\nu)$ is bounded, then*

$$\check{\Lambda}_k = \sum_{q=-\infty}^{k-1} \sum_{s=-\infty}^{q-1} e^{-a(k-s-2)h}\check{z}_s \in \mathbb{ERG}(\mathbb{Z},\mathbb{L}^2(\mathbb{P},\mathbb{R}),\mu,\nu), \quad \forall k \in \mathbb{Z},$$

where $\hat{z} \in \mathbb{W}^2\mathbb{AP}^{\vartheta}(\mathbb{Z},\mathbb{L}^2(\mathbb{P},\mathbb{R}))$, $\check{z} \in \mathbb{ERG}(\mathbb{Z},\mathbb{L}^2(\mathbb{P},\mathbb{R}),\mu,\nu)$.

Together with Propositions 3.6 and 3.7, we have:

Proposition 3.8. *If $a > 0$ and $z = \hat{z} + \check{z} \in \mathbb{W}^2\mathbb{PAP}^{\vartheta}(\mathbb{Z},\mathbb{L}^2(\mathbb{P},\mathbb{R}),\mu,\nu)$ is bounded, then*

$$\Lambda_k = \sum_{q=-\infty}^{k-1} \sum_{s=-\infty}^{q-1} e^{-a(k-s-2)h}z_s \in \mathbb{W}^2\mathbb{PAP}^{\vartheta}(\mathbb{Z},\mathbb{L}^2(\mathbb{P},\mathbb{R}),\mu,\nu), \quad \forall k \in \mathbb{Z},$$

where $\hat{z} \in \mathbb{W}^2\mathbb{AP}^{\vartheta}(\mathbb{Z},\mathbb{L}^2(\mathbb{P},\mathbb{R}))$, $\check{z} \in \mathbb{ERG}(\mathbb{Z},\mathbb{L}^2(\mathbb{P},\mathbb{R}),\mu,\nu)$.

3.2. MS-(μ,ν)-PWAPS

Let $\mathscr{D}_*$ be some bounded open set in $\mathbb{R}^N$, $F \in C(\bar{\mathscr{D}}_*,\mathbb{R}^N)$, and $0 \in \mathbb{R}^N \setminus F(\partial\mathscr{D}_*)$. Define the Brouwer degree $\deg(F,\mathscr{D}_*,0)$ by $\deg(F,\mathscr{D}_*,0) := \deg(F_*,\mathscr{D}_*,0) = \sum_{x\in F_*^{-1}(0)} \mathrm{sgn}J_{F_*(x)}$, where $F_* \in C^2(\bar{\mathscr{D}}_*,\mathbb{R}^N)$ with

$\|F - F_*\| < \text{dist}(0, F(\partial\mathscr{D}_*))$, and $J_{F_*(x)}$ represents the Jacobian of F_* at the point $x \in \mathscr{D}_*$. Let $\mathbb{X}$ be a real Banach space, $\mathscr{D}_* \subseteq \mathbb{X}$ be an open bounded set, and $\Phi : \mathscr{D}_* \to \mathbb{X}$ be a continuous compact mapping. Now, suppose that $0 \notin (I - \Phi)(\partial\mathscr{D}_*)$. Then there exists $\epsilon_0 > 0$ such that $x \neq t\Phi_{\epsilon_1}x + (1 - t)\Phi_{\epsilon_2}x, \forall t \in [0, 1], x \in \partial\mathscr{D}_*$, where $\epsilon_i \in (0, \epsilon_0)$, $\Phi_{\epsilon_i} : \bar{\mathscr{D}}_* \to F_{\epsilon_i}$, and F_{ϵ_i} denotes some finite dimensional space, $i = 1, 2$. Hence, we define the Leray Schauder degree by $\deg(I - \Phi, \mathscr{D}_*, 0) = \deg(I - \Phi_\epsilon, \mathscr{D}_* \cap F_\epsilon, 0)$, where F_ϵ is some finite dimensional space and $\epsilon \in (0, \epsilon_0)$.

Lemma 3.1 ([45, Theorem 2.2.4])**.** *The following properties of the Leray Schauder degree hold.*

1) (Normality). $\deg(I, \mathscr{D}_*, 0) = 1$ *if and only if* $0 \in \mathscr{D}_*$*;*

2) (Solvability). *If* $\deg(I - \Phi, \mathscr{D}_*, 0) \neq 0$*, then* $\Phi x = x$ *has a solution in* $\mathscr{D}_*$*;*

3) (Homotopy). *Let* $H_t(x) : [0, 1] \times \mathscr{D}_* \to \mathbb{X}$ *be continuous compact and* $H_t(x) \neq x$ *for all* $(t, x) \in [0, 1] \times \partial\mathscr{D}_*$*. Then* $\deg(I - H_t(\cdot), \mathscr{D}_*, 0)$ *does not depend on* $t \in [0, 1]$.

Appendix B contains the proofs of the theorems presented below.

Theorem 3.1. *Let conditions* (i_1)–(i_4) *be fulfilled. Then SINN* (2.1) *admits a mean-squared* (μ, ν)*-pseudo Weyl almost periodic sequence in* $\mathscr{D}_*$ *if*

$$(i_5)\ \ \mathfrak{R}_* := \max_{1\le i\le n} \frac{4}{a_i^2}\Big[\frac{4|\gamma_i|}{\hbar^2} + \bar{b}_i + \sum_{j=1}^{n} \bar{c}_{ij}L_j^f + \frac{1}{\sqrt{h}}\sum_{j=1}^{n} \bar{\xi}_{ij}L_{j*}^{\sigma}\Big] < 1.$$

By Theorem 3.1, SINN (2.1) possesses a mean-squared (μ, ν)-pseudo Weyl almost periodic sequence solution $\tilde{\mathbf{z}} = (\tilde{z}_1, \tilde{z}_2, \ldots, \tilde{z}_n)^T$. Define the initial values of SINN (2.1) by

$$z_{i,s}^{[\iota]} = \tilde{z}_{i,s}^{[\iota]}, \quad \forall(\iota, s) \in (0, \aleph)_{\mathbb{Z}} \times [-\delta_\infty, 1]_{\mathbb{Z}}, i = 1, 2, \ldots, n. \tag{3.2}$$

Theorem 3.2. *Let conditions* (i_1)–(i_5) *be fulfilled. Then SINN* (2.1) *admits a unique mean-squared* (μ, ν)*-pseudo Weyl almost periodic sequence with the initial values* (3.2)*.*

Remark 3.1. *Previous studies, such as [6, 13], have explored periodic behaviors in INNs, including random periodicity [6] and weighted pseudo-almost periodic sequences [13]. While these works laid foundational insights, our research advances the field in two significant directions. 1) We introduce, for the first time, the concept of random ergodic Weyl almost periodicity for space-time differencing INNs (*Theorem 3.1*). This extends the classical framework of almost periodicity to stochastic settings, addressing a critical gap in the analysis of discrete spatiotemporal neural systems. Our approach leverages ergodic theory and Weyl metrics to characterize recurrent patterns under noise, generalizing existing results on deterministic periodicity [20–22]. 2) We rigorously analyze the impact of Euler-Maruyama noise on INN dynamics. Unlike prior works that focused solely on deterministic models, our study incorporates stochastic partial difference equations (SPDEs) to model noise propagation, offering practical guidelines for parameter design.*

4. Exponential stabilization and stability under stochastic disturbances

This section explores the global exponential stabilization and stability of SINNs in a discrete space-time framework. By introducing feedback control strategies, this section provides the first proof of

global exponential stabilization. Theoretical analysis shows that increasing control coefficients accelerates system convergence, but excessive control may lead to instability. Numerical experiments further validate the theoretical results, offering theoretical support for analyzing complex dynamic behaviors in neuromorphic computing and biological neural modeling. Additionally, when the diffusion term is zero, the system remains globally exponentially stable, highlighting the synergistic role of damping parameters and control design.

For $\kappa_i > 0$, similar to Lemma 2.1 of paper [13], SINN (2.1) can be decomposed as

$$\begin{cases} \Delta z_{i,k}^{[\iota]} = \kappa_i(e^{-\frac{1}{2}a_i h} - 1)z_{i,k}^{[\iota]} + \alpha_i w_{i,k}^{[\iota]}, \\ \Delta w_{i,k}^{[\iota]} = (e^{-\frac{1}{2}a_i h} - 1)w_{i,k}^{[\iota]} + \alpha_i\Big[\gamma_i\Delta_\iota^2 z_{i,k}^{[\iota]} + (\dfrac{\kappa_i a_i^2}{4} - b_{i,k})z_{i,k}^{[\iota]} \\ \qquad\qquad + \displaystyle\sum_{j=1}^{n} c_{ij,k}f_j(z_{j,k-\delta_{j,k}}^{[\iota]}) + \frac{1}{\sqrt{h}}\sum_{j=1}^{n}\xi_{ij,k}\sum_{l=1}^{\infty}\sigma_{jl}(z_{j,k-o_{j,k}}^{[\iota]})\varepsilon_{l,k} + I_{i,k}\Big], \end{cases} \tag{4.1}$$

where $(\iota, k) \in (0, \aleph)_{\mathbb{Z}} \times \mathbb{Z}_0$, $i = 1, 2, \ldots, n$.

Supposing that all assumptions in Theorem 3.2 hold, then SINN (2.1) has a unique mean-squared (μ, ν)-pseudo Weyl almost periodic sequence $\tilde{\mathbf{z}} = (\tilde{z}_1, \tilde{z}_2, \ldots, \tilde{z}_n)^T$ satisfying $\Delta\tilde{z}_{i,k}^{[\iota]} = \kappa_i(e^{-\frac{1}{2}a_i h} - 1)\tilde{z}_{i,k}^{[\iota]} + \alpha_i\tilde{w}_{i,k}^{[\iota]}$, where $\tilde{\mathbf{w}} = (\tilde{w}_1, \tilde{w}_2, \ldots, \tilde{w}_n)^T$ fulfills

$$\begin{aligned} \Delta\tilde{w}_{i,k}^{[\iota]} = (e^{-\frac{1}{2}a_i h} - 1)\tilde{w}_{i,k}^{[\iota]} + \alpha_i\Big[\gamma_i\Delta_\iota^2\tilde{z}_{i,k}^{[\iota]} + (\frac{\kappa_i a_i^2}{4} - b_{i,k})\tilde{z}_{i,k}^{[\iota]} \\ + \sum_{j=1}^{n} c_{ij,k}f_j(\tilde{z}_{j,k-\delta_{j,k}}^{[\iota]}) + \frac{1}{\sqrt{h}}\sum_{j=1}^{n}\xi_{ij,k}\sum_{l=1}^{\infty}\sigma_{jl}(\tilde{z}_{j,k-o_{j,k}}^{[\iota]})\varepsilon_{l,k} + I_{i,k}\Big] \end{aligned} \tag{4.2}$$

for all $(\iota, k) \in (0, \aleph)_{\mathbb{Z}} \times \mathbb{Z}$, $i = 1, 2, \ldots, n$. Furthermore, $\tilde{z}_{i,k}^{[\iota]}\Big|_{\iota\in\{0,\aleph\}} = 0 = \tilde{w}_{i,k}^{[\iota]}\Big|_{\iota\in\{0,\aleph\}}$, $\forall k \in \mathbb{Z}$, $i = 1, 2, \ldots, n$.

Considering the control inputs in SINN (4.1), it becomes

$$\begin{cases} \Delta z_{i,k}^{[\iota]} = \kappa_i(e^{-\frac{1}{2}a_i h} - 1)z_{i,k}^{[\iota]} + \alpha_i w_{i,k}^{[\iota]}, \\ \Delta w_{i,k}^{[\iota]} = (e^{-\frac{1}{2}a_i h} - 1)w_{i,k}^{[\iota]} + \alpha_i\Big[\gamma_i\Delta_\iota^2 z_{i,k}^{[\iota]} + (\dfrac{\kappa_i a_i^2}{4} - b_{i,k})z_{i,k}^{[\iota]} \\ \qquad\qquad + \displaystyle\sum_{j=1}^{n} c_{ij,k}f_j(z_{j,k-\delta_{j,k}}^{[\iota]}) + \frac{1}{\sqrt{h}}\sum_{j=1}^{n}\xi_{ij,k}\sum_{l=1}^{\infty}\sigma_{jl}(z_{j,k-o_{j,k}}^{[\iota]})\varepsilon_{l,k} + I_{i,k}\Big] + \rho_{i,k}^{[\iota]}, \end{cases} \tag{4.3}$$

where $\rho_{i,k}^{[\iota]}$ denotes the feedback controls, $(\iota, k) \in (0, \aleph)_{\mathbb{Z}} \times \mathbb{Z}_0$, $i = 1, 2, \ldots, n$. Define

$$z_{i,s}^{[\iota]} = \varphi_{i,s}^{[\iota]},\ w_{i,s}^{[\iota]} = \phi_{i,s}^{[\iota]}, \quad \forall(\iota, s) \in (0, \aleph)_{\mathbb{Z}} \times [-\delta_\infty, 0]_{\mathbb{Z}}; \quad z_{i,k}^{[\iota]}\Big|_{\iota\in\{0,\aleph\}} = 0 = w_{i,k}^{[\iota]}\Big|_{\iota\in\{0,\aleph\}},$$

$\forall k \in \mathbb{Z}_0$, $i = 1, 2, \ldots, n$. We design the feedback controls in SINN (4.3) by

$$\rho_{i,k}^{[\iota]} = \mathscr{a}_i(w_{i,k}^{[\iota]} - \tilde{w}_{i,k}^{[\iota]}), \quad \forall(\iota, k) \in (0, \aleph)_{\mathbb{Z}} \times \mathbb{Z}_0, i = 1, 2, \ldots, n. \tag{4.4}$$

Suppose that

(i_6) $\kappa_i := \dfrac{e^{-\frac{1}{2}\eta_i h} - 1}{e^{-\frac{1}{2}a_i h} - 1}$, $\mathscr{a}_i := e^{-\frac{1}{2}\mathscr{d}_i h} - e^{-\frac{1}{2}a_i h}$, where $\eta_i > 0$, $\mathscr{d}_i > 0$, $i = 1, 2, \ldots, n$.

Based on (4.1)–(4.4) and condition (i_6), we have

$$\begin{cases} x_{i,k+1}^{[\iota]} = e^{-\frac{1}{2}\eta_i h} x_{i,k}^{[\iota]} + \alpha_i y_{i,k}^{[\iota]}, \\ y_{i,k+1}^{[\iota]} = e^{-\frac{1}{2}\mathscr{A}_i h} y_{i,k}^{[\iota]} + \alpha_i \Big\{ \gamma_i \Delta_\iota^2 x_{i,k}^{[\iota]} + (\frac{\kappa_i a_i^2}{4} - b_{i,k}) x_{i,k}^{[\iota]} + \sum_{j=1}^{n} c_{ij,k} \Big[f_j(z_{j,k-\delta_{j,k}}^{[\iota]}) - f_j(\tilde{z}_{j,k-\delta_{j,k}}^{[\iota]}) \Big] \\ \qquad + \frac{1}{\sqrt{h}} \sum_{j=1}^{n} \xi_{ij,k} \sum_{l=1}^{\infty} \Big[\sigma_{jl}(z_{j,k-o_{j,k}}^{[\iota]}) - \sigma_{jl}(\tilde{z}_{j,k-o_{j,k}}^{[\iota]}) \Big] \varepsilon_{l,k} \Big\}, \quad \forall (\iota, k) \in (0, \aleph)_{\mathbb{Z}} \times \mathbb{Z}_0, \\ x_{i,s}^{[\iota]} = \varphi_{i,s}^{[\iota]} - \tilde{z}_{i,s}^{[\iota]}, \ y_{i,s}^{[\iota]} = \phi_{i,s}^{[\iota]} - \tilde{w}_{i,s}^{[\iota]}, \quad \forall (\iota, s) \in (0, \aleph)_{\mathbb{Z}} \times [-\delta_\infty, 0]_{\mathbb{Z}}, \\ x_{i,k}^{[\iota]}\Big|_{\iota \in \{0,\aleph\}} = 0 = y_{i,k}^{[\iota]}\Big|_{\iota \in \{0,\aleph\}}, \quad \forall k \in \mathbb{Z}_0, \end{cases} \tag{4.5}$$

where $x_i = z_i - \tilde{z}_i$, $y_i = w_i - \tilde{w}_i$, $i = 1, 2, \ldots, n$. Let $x = (x_1, x_2, \ldots, x_n)^T$, $y = (y_1, y_2, \ldots, y_n)^T$, and $F := \max_{1 \le i \le n} \max_{(\iota,s) \in (0,\aleph)_{\mathbb{Z}} \times [-\delta_\infty, 0]_{\mathbb{Z}}} \{ \|\varphi_{i,s}^{[\iota]} - \tilde{z}_{i,s}^{[\iota]}\|_2 + \|\phi_{i,s}^{[\iota]} - \tilde{w}_{i,s}^{[\iota]}\|_2 \}$. Define $\hat{b}_i := \sup_{k \in \mathbb{Z}} \left| \frac{\kappa_i}{4} a_i^2 - b_{i,k} \right|$, where $i, j = 1, 2, \ldots, n$.

Definition 4.1. *Under the feedback control* (4.4)*, SINN* (2.1) *is said to be globally exponentially stabilized to MS-WPAPS* $\tilde{\mathbf{z}} = (\tilde{z}_1, \tilde{z}_2, \ldots, \tilde{z}_n)^T$ *if there exist constants* $\mathscr{U} > 1$ *and* $\varpi > 0$ *such that*

$$\|x_k\|_* \le \mathscr{U} F e^{-\varpi k h}, \quad \forall k \in \mathbb{Z}_0. \tag{4.6}$$

If $\gamma \equiv 0$ *in SINN* (4.3)*, and inequality* (4.6) *holds, then MS-WPAPS* $\tilde{\mathbf{z}} = (\tilde{z}_1, \tilde{z}_2, \ldots, \tilde{z}_n)^T$ *in SINN* (2.1) *is said to be globally exponentially stable.*

The detailed proof of the following theorem is provided in Appendix B.

Theorem 4.1. *Suppose that* (i_1)–(i_6) *and the following hypothesis hold.*

(i_7) $\max\limits_{1 \le i \le n} \left\{ \dfrac{\alpha_i}{1 - e^{-\frac{1}{2}\eta_i h}}, \dfrac{\alpha_i \mathscr{L}_i}{1 - e^{-\frac{1}{2}\mathscr{A}_i h}} \right\} < 1$, *where* $\mathscr{L}_i = \frac{4}{\hbar^2}|\gamma_i| + \hat{b}_i + \sum_{j=1}^{n} \bar{c}_{ij} L_j^f + \frac{1}{\sqrt{h}} \sum_{j=1}^{n} \bar{\xi}_{ij} L_{j*}^{\sigma}$.

Then SINN (2.1) *is globally exponentially stabilized to MS-WPAPS* $\tilde{\mathbf{z}} = (\tilde{z}_1, \tilde{z}_2, \ldots, \tilde{z}_n)^T$ *via the feedback control* (4.4)*, which has the exponential convergence rate* $0 < \varpi = \varpi(\mathscr{U}) < \frac{1}{2} \min\{\eta_i, \mathscr{A}_i\}$ *satisfying*

$$\frac{1}{\mathscr{U}} + \max_{1 \le i \le n} \left\{ \frac{\alpha_i e^{\varpi h}}{1 - e^{-(\frac{1}{2}\eta_i - \varpi)h}}, \frac{\alpha_i e^{\varpi(\delta_\infty + 1)h}}{1 - e^{-(\frac{1}{2}\mathscr{A}_i - \varpi)h}} \mathscr{L}_i \right\} < 1.$$

Letting $\eta_i = \mathscr{A}_i = a_i$ in (i_6), then the control (4.4) is invalid and (i_7) is changed into

(i_8) $\max\limits_{1 \le i \le n} \left\{ \dfrac{2}{a_i}, \dfrac{2}{a_i} \Big[\dfrac{4}{\hbar^2}|\gamma_i| + \bar{b}_i + \sum_{j=1}^{n} \bar{c}_{ij} L_j^f + \dfrac{1}{\sqrt{h}} \sum_{j=1}^{n} \bar{\xi}_{ij} L_{j*}^{\sigma} \Big] \right\} < 1.$

According to Theorem 4.1, we have the following result of global exponential stability.

Theorem 4.2. *Suppose that* (i_1)–(i_5) *and* (i_8) *hold. Then MS-WPAPS* $\tilde{\mathbf{z}} = (\tilde{z}_1, \tilde{z}_2, \ldots, \tilde{z}_n)^T$ *in SINN* (2.1) *is globally exponentially stable.*

Remark 4.1. *Previous studies on stability in INNs, such as [27–29], have primarily focused on deterministic models or continuous-time systems, employing methods like Lyapunov functions and reduced-order techniques. Our work advances this field by introducing a novel framework for the global exponential stabilization of discrete space-time SINNs under Euler-Maruyama noise. Specifically: 1) We*

propose feedback control strategies tailored for SINNs, achieving stabilization despite time-delay and stochastic disturbances. This extends existing control theories (e.g., [32–34]) to high-dimensional, nonlinear, and stochastic discrete systems. 2) Our analysis reveals a critical trade-off: increasing control coefficients accelerates convergence, but excessive control leads to instability, providing practical design guidelines absent in prior works like [34, 35]. These contributions address gaps in both theoretical analysis and practical applications, advancing the understanding of complex neural systems under stochastic influences. The findings are relevant to report [5], where robust control and stability are essential for ensuring the reliability of safety-critical systems.

Remark 4.2. *Although Lyapunov-based techniques are employed in the stability analysis, several mechanisms are incorporated to reduce the conservatism of the derived criteria. First, the non-decomposed constant variation formula preserves the intrinsic coupling structure of the discrete inertial reaction–diffusion system, avoiding additional estimation layers caused by system decomposition. Second, the exponential Euler difference scheme provides a more accurate discrete representation of the continuous-time dynamics, thereby reducing discretization-induced conservatism. Furthermore, the stability conditions are parameter-dependent rather than uniformly bounded, which enlarges the admissible parameter region. Therefore, the obtained sufficient conditions are less restrictive compared with conventional coarse inequality-based approaches.*

Reliability-oriented interpretation of the theoretical results

The stability conditions derived in Theorems 3.2 and 4.2 not only guarantee the mathematical well-posedness of the discrete stochastic inertial neural network (SINN) but also provide quantitative indicators for system reliability and safety. From a reliability engineering viewpoint, the mean-square (μ, ν)-pseudo Weyl almost periodic solution (MS-(μ, ν)-PWAPS) can be interpreted as the stochastic analogue of a *safe operational regime* under uncertainty. Specifically:

- The mean-square boundedness of network states implies that the probability of unsafe deviations (e.g., component overload or control saturation) remains below a prescribed threshold. Hence, it can be regarded as an upper bound on the instantaneous *failure probability*.
- The exponential convergence rate established in Theorem 4.1 characterizes the system's *resilience*, representing the rate at which stochastic disturbances decay and the system returns to its nominal safe state. This provides a quantitative measure of the *reliability margin*. Further, the exponential convergence rate can be solved by the following optimal problem for each $\mathscr{U} > 1$:

$$\begin{aligned} &\max\ \varpi \\ &s.t.\ \ 0 < \varpi < \frac{1}{2}\min\{\eta_i, \mathscr{A}_i\}; \\ &\qquad \frac{1}{\mathscr{U}} + \frac{\alpha_i e^{\varpi h}}{1 - e^{-(\frac{1}{2}\eta_i - \varpi)h}} < 1; \\ &\qquad \frac{1}{\mathscr{U}} + \frac{\alpha_i e^{\varpi(\delta_\infty + 1)h}}{1 - e^{-(\frac{1}{2}\mathscr{A}_i - \varpi)h}}\mathscr{L}_i < 1, \quad 1 \le i \le n. \end{aligned}$$

- The parameter condition $\mathfrak{R}_* < 1$ defines a safety margin in parameter space: larger damping or diffusion coefficients increase this margin, whereas excessive delay or noise intensity reduce it.

Therefore, $\mathfrak{R}_*$ serves as a *stochastic safety index* linking mathematical stability with engineering reliability.

These mappings allow the theoretical results to be embedded into reliability assessment and decision-making processes. In particular, the derived inequalities can be used to evaluate the sensitivity of reliability with respect to control, diffusion, and delay parameters. The subsequent numerical simulations further demonstrate how these theoretical metrics translate into measurable reliability indicators such as bounded failure probability, resilience, and fatigue-safe operation in robotic systems.

5. Numerical experiment: Robust robotic joint control

To illustrate the engineering relevance and reliability implications of the proposed SINN framework, we conduct comprehensive numerical experiments on a robotic joint system—a representative example of a safety-critical mechatronic subsystem operating under stochastic disturbances and communication delays, see Figure 1. This system provides a realistic platform for evaluating how the theoretical results translate into measurable reliability-oriented performance indicators such as bounded failure probability, stability margin, and fatigue-safe operation.

In this context, *reliability* refers to the probability that the system remains within its safe operational envelope despite random perturbations, while *resilience* denotes the rate at which the system recovers from deviations. The discrete-time SINN model allows us to interpret the mean-square (μ, ν)-pseudo Weyl almost periodic sequence (MS-(μ, ν)-PWAPS) solution as a statistical descriptor of long-term safe operation under uncertainty. Specifically, the mean-square boundedness of joint states corresponds to a low probability of unsafe oscillations, and the exponential convergence rate provides a quantitative measure of the system's reliability margin.

The following simulations examine how diffusion strength, the damping coefficient, and control intensity affect reliability-oriented measures. For each parameter configuration, we evaluate:

1) the mean-square deviation from the nominal trajectory (serving as a proxy for failure probability);

2) the exponential convergence rate (reflecting resilience and recovery speed); and

3) the smoothness and amplitude of oscillations (linked to fatigue-life and safety margin).

By systematically varying these parameters, we identify the trade-offs between rapid convergence and reliability robustness. Stronger diffusion and damping enhance reliability by reducing oscillation amplitudes and lowering the likelihood of trajectory divergence, whereas excessive control gain—though accelerating convergence—can degrade stability and shorten fatigue life. These findings align with reliability-oriented controller design principles, emphasizing that stability, safety, and control performance must be jointly optimized.

The simulation results, presented in Figures 2–15, quantitatively validate the theoretical predictions: when the stability criterion $\mathfrak{R}_* < 1$ and condition (i_8) are satisfied, the system exhibits a unique MS-(μ, ν)-PWAPS that ensures reliable, near-periodic behavior. This outcome confirms that the proposed stochastic control strategy not only guarantees mathematical stability but also enhances operational reliability, offering a practical basis for risk-informed tuning of diffusion, damping, and control parameters in safety-critical robotic applications.

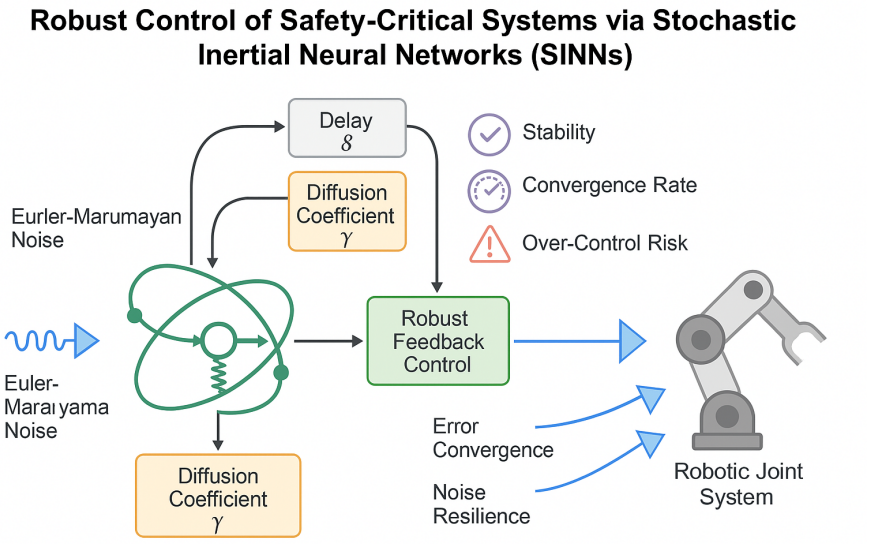

Figure 1. Robust control via SINNs.

To demonstrate the practical relevance of the proposed SINN model and its feedback control law, we consider a robotic manipulator with three actuated joints. Each network node $z_{i,k}^{[\iota]}$ represents the angular position of the i-th joint at discrete time k under internal index $i = 1, 2, 3$. The second-order difference $\Delta^2 z_{i,k}^{[\iota]}$ captures discrete joint acceleration (inertia), while the dissipation coefficient a_i models viscous friction and damping. Here, h denotes the digital sampling period, linking continuous joint dynamics to discrete implementation; $\hbar$ reflects the discretization resolution of the internal index, characterizing the granularity of event-triggered updates; $\gamma_i \Delta_\iota^2 z_{i,k}^{[\iota]}$ is a discrete diffusion term, representing interaction or averaging across internal indices (spatial or internal-layer diffusion); the coefficient γ_i scales the diffusion effect, controlling how strongly the joint state propagates across neighboring internal indices, analogous to diffusion in a discretized PDE; $b_{i,k}$ is a time-varying stiffness or feedback gain, used for stabilization or trajectory tracking; $c_{ij,k}$ denotes the coupling strength (possibly time-varying for coordinated motion); $f_j(\cdot)$ is a nonlinear activation or force mapping (e.g., saturation, dead-zone, or nonlinear stiffness models); $\xi_{ij,k}$ shows noise coupling coefficients (which joints' noise propagates to the current joint), and $\sigma_{jl}(\cdot)$ is the state-dependent noise intensity; $\delta_{j,k}$ and $o_{j,k}$ stand for the delays in information transmission (sensor/communication latency) and noise effect (e.g., actuator-induced lag), respectively. The nonlinear coupling term $\sum_{j=1}^{n} c_{ij,k} f_j(z_{j,k-\delta_{j,k}}^{[\iota]})$ represents joint interactions, and the multiplicative stochastic perturbation $\frac{1}{\sqrt{h}} \sum_{j=1}^{n} \xi_{ij,k} \sum_{l=1}^{\infty} \sigma_{jl}(z_{j,k-o_{j,k}}^{[\iota]}) \varepsilon_{l,k}$ accounts for state-dependent disturbances and measurement noise. The time-varying linear term $-(\frac{1}{4}a_i^2 + b_{i,k}) z_{i,k}^{[\iota]}$ serves as temporally modulated stiffness/feedback, and $I_{i,k}$ denotes reference torques from a high-level planner.

For simulations, the SINN parameters are set as $a = (4, 4.8, 4.4)$, $h = 0.2$, $\hbar = 0.5$, and $\gamma_1 = \gamma_2 = \gamma_3 = 0.1$, with internal indices $\iota = 1, 2, 3, 4$. Feedback gain $b_{i,k} = 0.1 \sin(k)$, joint interactions' term $c_{ij,k} f_j(z_{j,k-\delta_{j,k}}^{[\iota]}) = 0.1 \sin(z_{j,k-1}^{[\iota]})$, and the measurement noise $\xi_{ij,k} \sum_{l=1}^{\infty} \sigma_{jl}(z_{j,k-o_{j,k}}^{[\iota]}) = 0.1 \cos k \sum_{l=1}^{\infty} e^{-l} \sin^2(z_{j,k-1}^{[\iota]})$. Reference torques are $I_{1,k} = 0.12 \cos(\sqrt{2}k) + 0.13 \cos(\sqrt{3}k) + e^{-0.1|k|}$, $I_{2,k} = 0.1 \sin(\sqrt{5}k) + 0.14 \sin(\sqrt{7}k) + e^{-0.2|k|}$, $I_{3,k} =$

$0.2\cos(\sqrt{12}k) + 0.3\cos(\sqrt{13}k) + e^{-0.3|k|}$, combining oscillatory excitations with decaying components to mimic realistic actuation signals. Simulations are conducted over $k = 0, 1, \ldots$. Initial states are $z_{i,s}^{[\iota]} = i\iota + s\cos(\iota^2) + 10$ for $s = -1, 0, 1$, with boundary conditions $z_{i,k}^{[0]} = z_{i,k}^{[5]} = 0$. So, the SINN takes the form

$$\begin{cases} \Delta^2 z_{i,k}^{[\iota]} = 2(e^{-\frac{1}{2}a_i h} - 1)\Delta z_{i,k}^{[\iota]} + \left[\dfrac{2 - 2e^{-\frac{1}{2}a_i h}}{a_i}\right]^2 \Big[\gamma_i \Delta_\iota^2 z_{i,k}^{[\iota]} - \Big(\dfrac{1}{4}a_i^2 + 0.1\sin(k)\Big) z_{i,k}^{[\iota]} \\ \qquad\qquad + 0.1\displaystyle\sum_{j=1}^{3} \sin(z_{j,k-1}^{[\iota]}) + \frac{0.1\cos k}{\sqrt{h}} \sum_{j=1}^{3}\sum_{l=1}^{\infty} \sin^2(z_{j,k-1}^{[\iota]}) e^{-l}\varepsilon_{l,k} + I_{i,k}\Big], k = 0, 1, 2, \ldots, \\ z_{i,s}^{[\iota]} = i\iota + s\cos(\iota^2) + 10, \quad s = -1, 0, 1, i = 1, 2, 3, \\ z_{i,k}^{[0]} = 0 = z_{i,k}^{[5]}, \quad k = 0, 1, 2, \ldots, \end{cases} \tag{5.1}$$

where $\iota = 1, 2, 3, 4$.

All assumptions stipulated in Theorem 3.1 are satisfied, with the critical parameter in condition (i_5), $\mathfrak{R}_* = 0.4862 < 1$, confirming the applicability of the theoretical framework to the robotic joint control scenario. Based on Theorems 3.1 and 3.2, system (5.1) admits a unique mean-square (μ, ν)-pseudo MS-(μ, ν)-PWAPS, which quantitatively characterizes the long-term approximate periodicity of joint angles in the presence of stochastic disturbances and delays, as demonstrated in Figures 2–10. This sequence provides a rigorous tool for predicting average joint positions and dynamic behavior over prolonged or repetitive robotic tasks, which is crucial for trajectory planning, fatigue analysis, and safe manipulator operation.

Figures 2–9 depict the two-dimensional PWAPS trajectories of the robotic joint states under different diffusions and damping parameters. The simulations clearly show that a stronger diffusion strength or damping reduces oscillation amplitudes and yields smoother trajectories, highlighting the homogenizing role of diffusive coupling and viscous damping. These results are consistent with the theoretical analysis, demonstrating that properly tuned diffusion and damping enhance synchronization, suppress stochastic fluctuations, and ultimately improve the reliability of robotic joint motion. From an engineering perspective, such dynamics are crucial for safety-critical applications—where unpredictable disturbances could otherwise compromise stability—and suggest a direct pathway for parameter tuning in the design of reliable robotic manipulators. Figure 10 further provides a three-dimensional visualization of the PWAPS across all joints, offering a comprehensive view of the spatiotemporal regularity in joint motion. Together, these results validate the proposed framework as an effective tool for capturing long-term statistical patterns in robotic trajectories under noise and delays. Importantly, they also bridge the theoretical foundation with practical engineering implications, supporting reliability-oriented tasks such as trajectory planning, fatigue life estimation, and safe manipulator operation.

Furthermore, condition (i_8) holds with the left-hand side of the associated inequality evaluated at $0.9724 < 1$, validating Theorem 4.2. Consequently, system (5.1) achieves global exponential stability in both two- and three-dimensional representations, confirming that the proposed strategy effectively stabilizes joint trajectories despite random disturbances and communication delays.

Building upon the attenuation and quasi-periodic regularities illustrated in Figures 2–15 further demonstrates the global exponential stability of the discrete SINN system in the absence of external controllers, even when subject to Euler–Maruyama noise and time delays. These figures show the state trajectories of three representative robotic joints initialized from different starting conditions. As time progresses, all solution curves converge exponentially toward the unique PWAPS. This behavior verifies

that the intrinsic dynamics of the system, governed by diffusion and damping, are sufficient to enforce robust stability despite stochastic disturbances and communication delays.

From an engineering standpoint, this intrinsic stability is of critical importance. It ensures that robotic joint motions naturally settle into predictable, near-periodic patterns without requiring continuous external intervention, providing a reliability baseline for safety-critical operations. Such predictable behavior is essential for tasks such as trajectory tracking, fatigue-life assessment, and maintaining safe manipulator performance under uncertain operating conditions. Moreover, the validation of global exponential stability for the uncontrolled system complements the theoretical results, confirming that the PWAPS framework not only captures long-term statistical regularities but also delivers fundamental insights into the inherent reliability of complex robotic systems. This sets the stage for the subsequent analysis, where the introduction of external controllers is shown to further enhance stabilization performance and operational robustness.

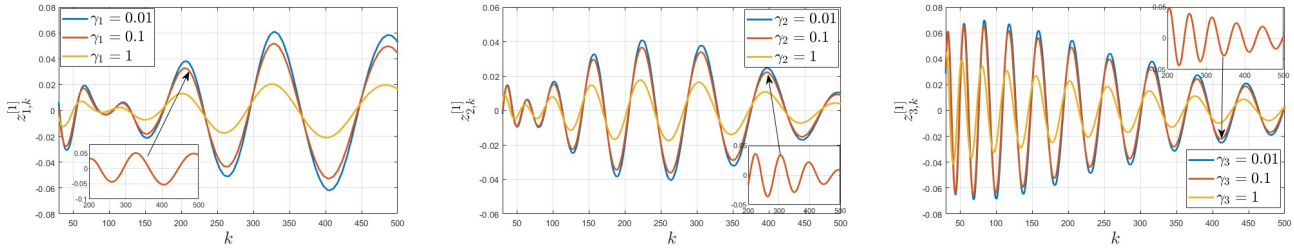

Figure 2. Ergodic Weyl almost periodic sequences ($z^{[1]}_{1\to 3,k}$) with different diffusions.

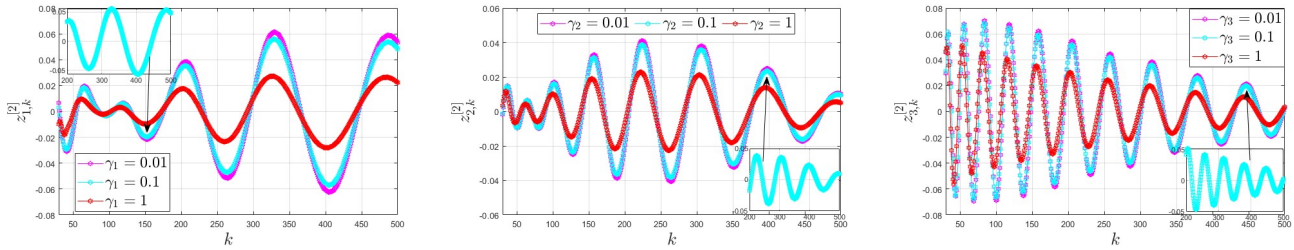

Figure 3. Ergodic Weyl almost periodic sequences ($z^{[2]}_{1\to 3,k}$) with different diffusions.

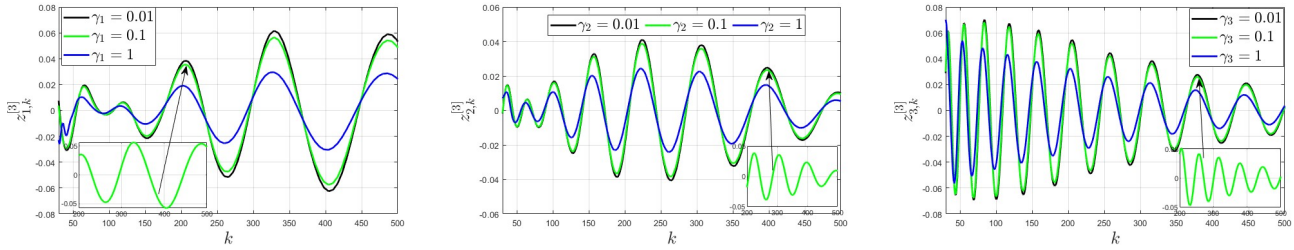

Figure 4. Ergodic Weyl almost periodic sequences ($z^{[3]}_{1\to 3,k}$) with different diffusions.

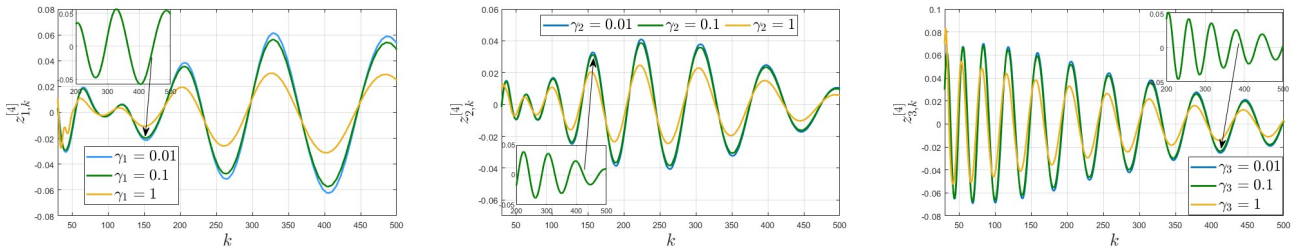

Figure 5. Ergodic Weyl almost periodic sequences $(z^{[4]}_{1\to 3,k})$ with different diffusions.

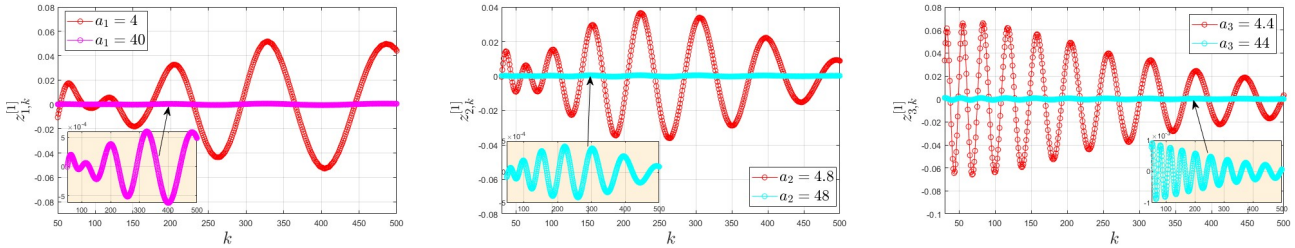

Figure 6. Ergodic Weyl almost periodic sequences $(z^{[1]}_{1\to 3,k})$ with different dampings.

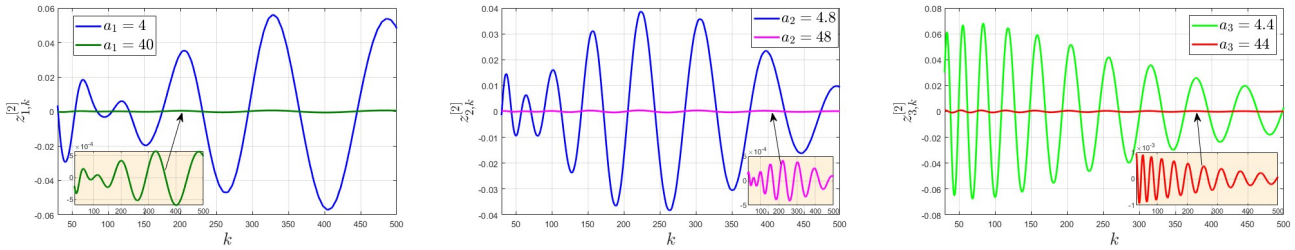

Figure 7. Ergodic Weyl almost periodic sequences $(z^{[2]}_{1\to 3,k})$ with different dampings.

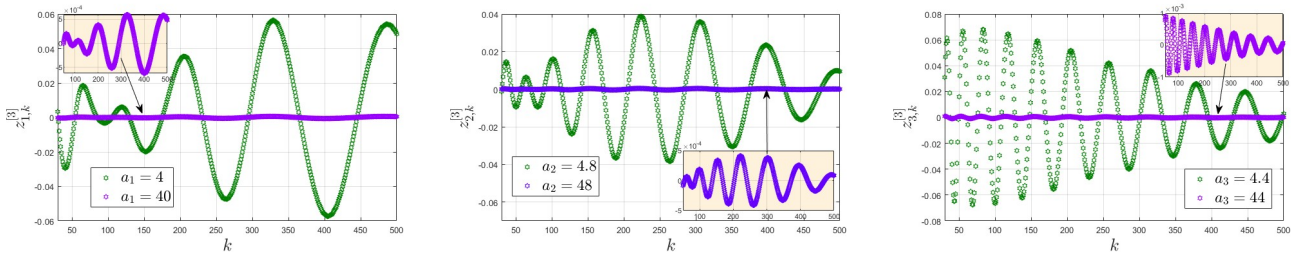

Figure 8. Ergodic Weyl almost periodic sequences $(z^{[3]}_{1\to 3,k})$ with different dampings.

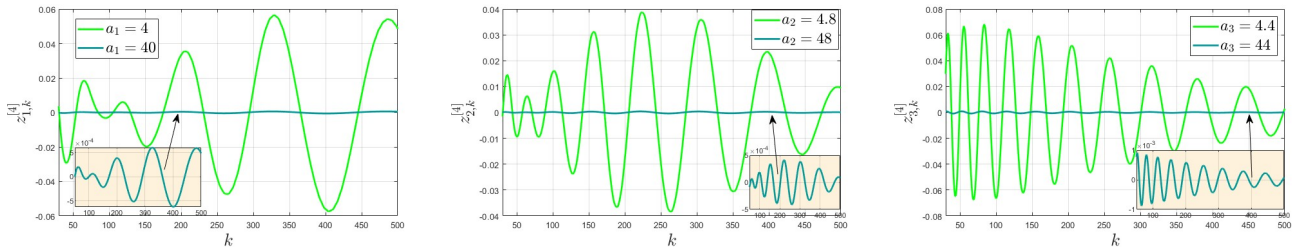

Figure 9. Ergodic Weyl almost periodic sequences $(z^{[4]}_{1\to 3,k})$ with different dampings.

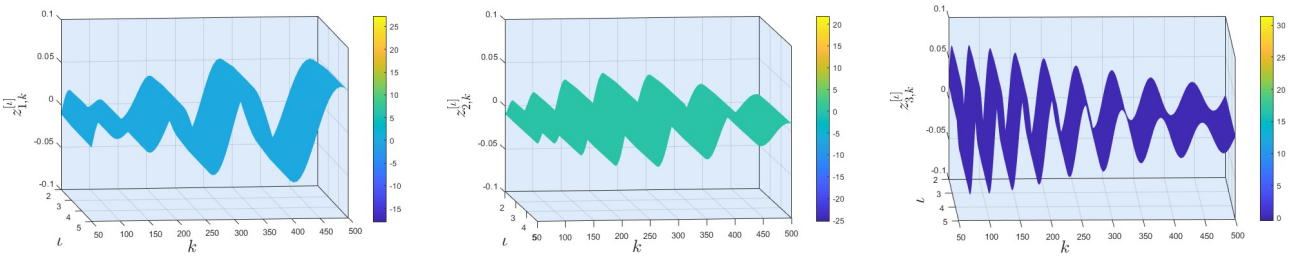

Figure 10. 3D plots of ergodic Weyl almost periodic sequences $(z_{1\to 3})$.

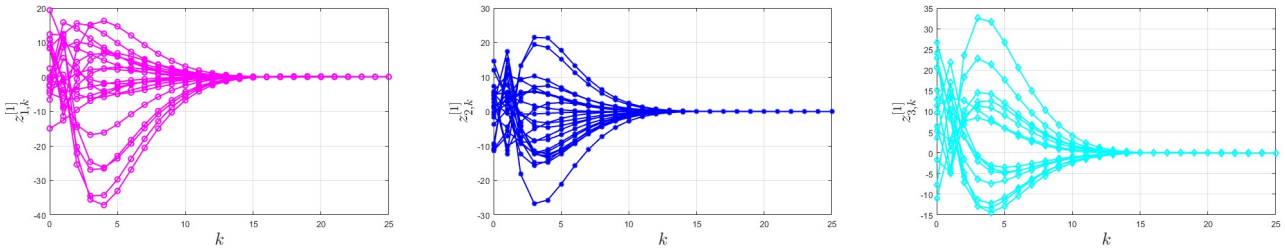

Figure 11. Global exponential stability $(z^{[1]}_{1\to 3,k})$ with initial values.

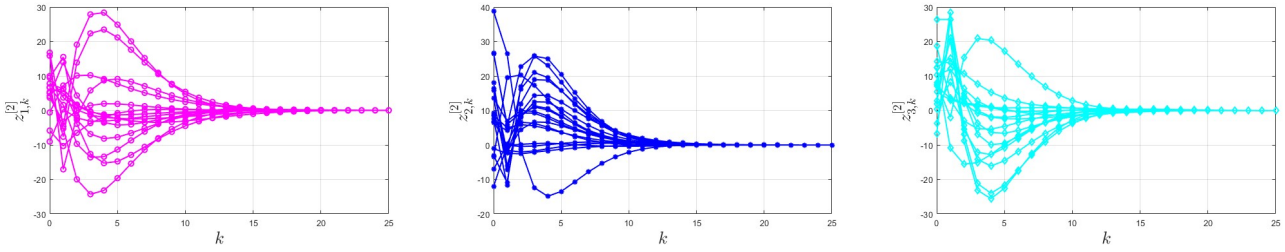

Figure 12. Global exponential stability $(z^{[2]}_{1\to 3,k})$ with initial values.

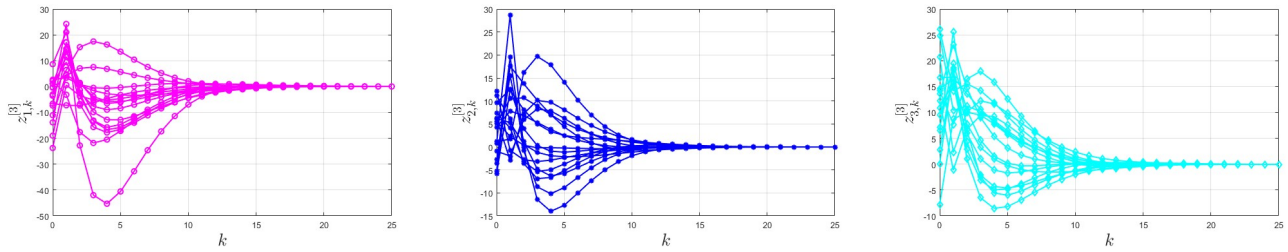

Figure 13. Global exponential stability ($z^{[3]}_{1\to3,k}$) with initial values.

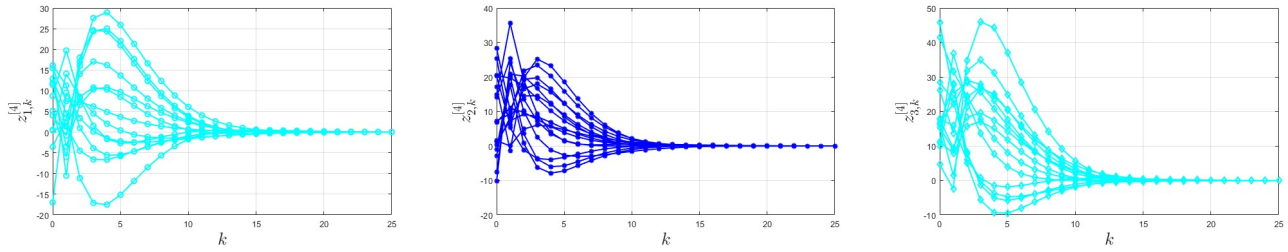

Figure 14. Global exponential stability ($z^{[4]}_{1\to3,k}$) with initial values.

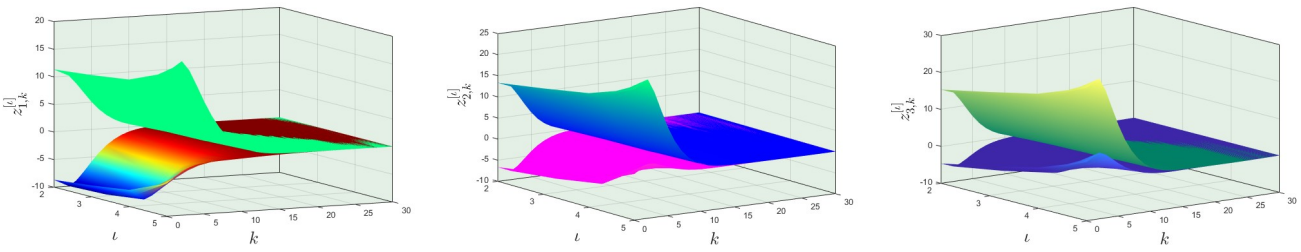

Figure 15. 3D plots of exponential stability ($z_{1\to3}$).

Considering the control inputs applied to SINN (5.1), the system is reformulated as the model below, where we set $a_i = \eta_i$ and $\mathscr{A}_i = d_i = 2a_i$ in condition (i_6).

$$\begin{cases} \Delta^2\tilde{z}^{[\iota]}_{i,k} = 2(e^{-\frac{1}{2}a_ih}-1)\Delta\tilde{z}^{[\iota]}_{i,k} + \left[\dfrac{2-2e^{-\frac{1}{2}a_ih}}{a_i}\right]^2\Big[\gamma_i\Delta^2_\iota\tilde{z}^{[\iota]}_{i,k} - \Big(\frac{1}{4}a_i^2 + 0.1\sin(k)\Big)\tilde{z}^{[\iota]}_{i,k} \\ \qquad\qquad + 0.1\sum_{j=1}^{3}\sin(\tilde{z}^{[\iota]}_{j,k-1}) + \dfrac{0.1\cos k}{\sqrt{h}}\sum_{j=1}^{3}\sum_{l=1}^{\infty}\sin^2(\tilde{z}^{[\iota]}_{j,k-1})e^{-l}\varepsilon_{l,k} + I_{i,k}\Big] + \rho^{[\iota]}_{i,k}, k = 0,1,2,\ldots, \\ \tilde{z}^{[\iota]}_{i,s} = i\iota + s\cos(\iota^2) - 10, \quad s = -1,0,1, i = 1,2,3, \\ \tilde{z}^{[0]}_{i,k} = 0 = \tilde{z}^{[5]}_{i,k}, \quad k = 0,1,2,\ldots, \end{cases} \tag{5.2}$$

where $\iota = 1,2,3,4$, and the feedback controls $\rho^{[\iota]}_{i,k}$ are defined by

$$\rho^{[\iota]}_{i,k} = \Big(e^{-\frac{1}{2}d_ih} - e^{-\frac{1}{2}a_ih}\Big)(w^{[\iota]}_{i,k} - \tilde{w}^{[\iota]}_{i,k}), \tag{5.3}$$

in which

$$\tilde{w}^{[\iota]}_{i,k} = \frac{1}{\alpha_i}\Delta\tilde{z}^{[\iota]}_{i,k} - \frac{1}{\alpha_i}(e^{-\frac{1}{2}a_ih}-1)\tilde{z}^{[\iota]}_{i,k}, \quad w^{[\iota]}_{i,k} = \frac{1}{\alpha_i}\Delta z^{[\iota]}_{i,k} - \frac{1}{\alpha_i}(e^{-\frac{1}{2}a_ih}-1)z^{[\iota]}_{i,k},$$

$\forall(\iota, k) \in (0,5)_{\mathbb{Z}} \times \mathbb{Z}_0, i = 1,2,3.$

Through calculation, condition (i_7) is satisfied with the left-hand side of the inequality evaluated as $0.5822 < 1$, validating the applicability of Theorem 4.1. Consequently, it is deduced that the Weyl almost periodic sequence of SINN (5.1) is globally exponentially stabilized by the feedback control law (5.3), as illustrated in Figures 16–19.

Figures 16–19 present the two-dimensional stabilized error trajectories of SINNs (5.1) and (5.2), under varying control coefficients $d = (d_1, d_2, d_3)$. These error signals are defined as $u_{1\to3,k}^{[1\to4]} = \tilde{z}_{1\to3,k}^{[1\to4]} - z_{1\to3,k}^{[1\to4]}$, where $\tilde{z}_{1\to3,k}^{[1\to4]}$ and $z_{1\to3,k}^{[1\to4]}$ represent the joint states at the k-th time step. The analysis of these error trajectories reveals a critical relationship between the control-to-damping ratio d/a (with a representing the damping parameter) and the system's stabilization behavior in robotic joint control.

a) When the ratio d/a increases from 1 to 2, the convergence rate of the error signals improves significantly. This indicates that stronger control inputs relative to damping accelerate the exponential suppression of errors, enabling the system to reach its stable state more rapidly. Such behavior is consistent with the theoretical predictions for controlled SINNs and demonstrates the capacity of the proposed feedback strategy to enhance stabilization efficiency. From an engineering perspective, this implies that robotic manipulators perform better when the control input is sufficiently strong to counteract random disturbances and delays.

b) However, when the ratio d/a exceeds a critical threshold (for instance, $d/a = 3$), the system becomes unstable. This is evidenced by divergent or oscillatory behavior of the error trajectories in the simulations, which demonstrates the over-control phenomenon. At this point, the feedback control surpasses the damping force, causing instability. This is critical for robotic joint control in real-world applications, as excessive control input can destabilize systems designed to maintain smooth, continuous motion. This finding emphasizes the need for careful calibration of the control parameters, especially in systems where precision and stability are paramount.

c) The consistent patterns across all simulations underscore the robustness of the stabilization strategy while revealing a fundamental trade-off between rapid convergence and long-term stability margins. This trade-off is especially relevant in safety-critical robotic systems, where rapid responsiveness is often desirable but cannot come at the expense of reliability and safety. Consequently, the results of Figures 16–19 provide actionable guidelines for the engineering design of feedback controllers, emphasizing the importance of parameter calibration to achieve reliable stabilization in uncertain and dynamic environments.

Figures 20–22 present the stabilization process of the robotic joint system in a three-dimensional state space, where the master and slave trajectories gradually converge under the action of the controller parameter ρ. A notable feature is that ρ decreases to zero as time progresses, fully consistent with the theoretical prediction: since ρ is directly driven by the synchronization error, the control input naturally vanishes once the error disappears. Compared with the earlier two-dimensional error trajectories, these three-dimensional visualizations provide a more comprehensive perspective on how the coupled joint dynamics achieve synchronization in the presence of noise and time delays. Importantly, they demonstrate that stability is not confined to a single trajectory but is instead a robust property of the entire multi-joint system, extending across different state dimensions.

From an engineering perspective, this insight is highly valuable. It shows that even under uncertain and dynamic environments, the proposed feedback mechanism ensures collective stability and coordination across subsystems. Such robustness is crucial for the design of fault-tolerant robotic joints, where deviations or failures in one component must not propagate to systemic instabilities. Moreover, the natural decay of the control input reflects an energy-efficient property of the strategy, ensuring that actuators are not continuously overloaded, which in turn prolongs system lifespan and reduces fatigue risks. Overall, the results of Figures 20–22 confirm the practical utility of the control framework for ensuring reliable, safe, and sustainable operation in safety-critical robotic applications.

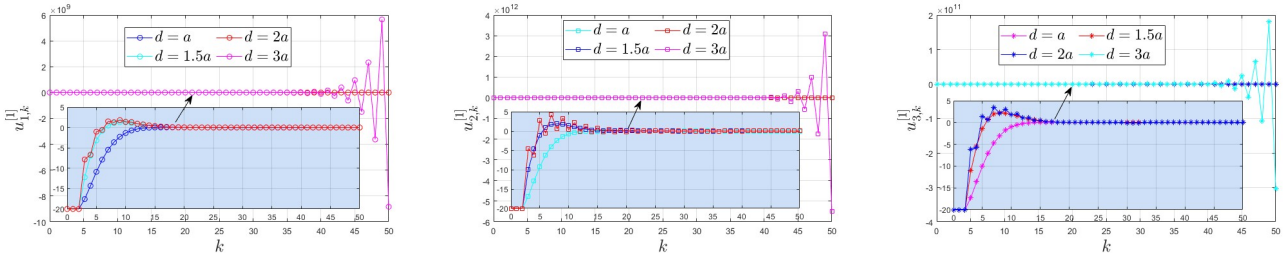

Figure 16. Exponential stabilization ($u_{1\to3,k}^{[1]}$) with different control coefficients.

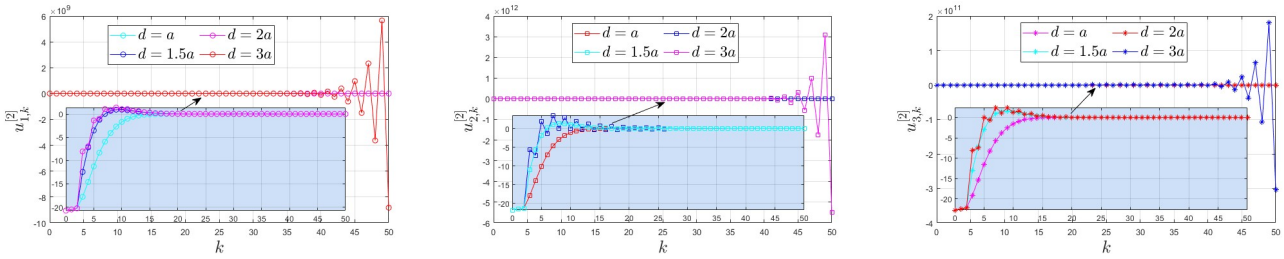

Figure 17. Exponential stabilization ($u_{1\to3,k}^{[2]}$) with different control coefficients.

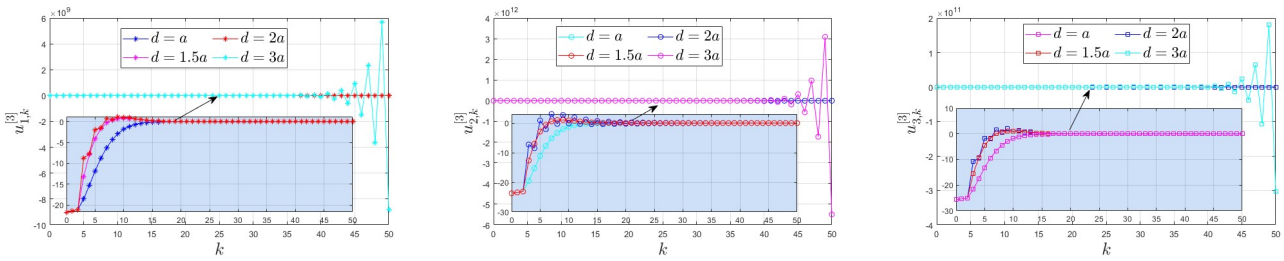

Figure 18. Exponential stabilization ($u_{1\to3,k}^{[3]}$) with different control coefficients.

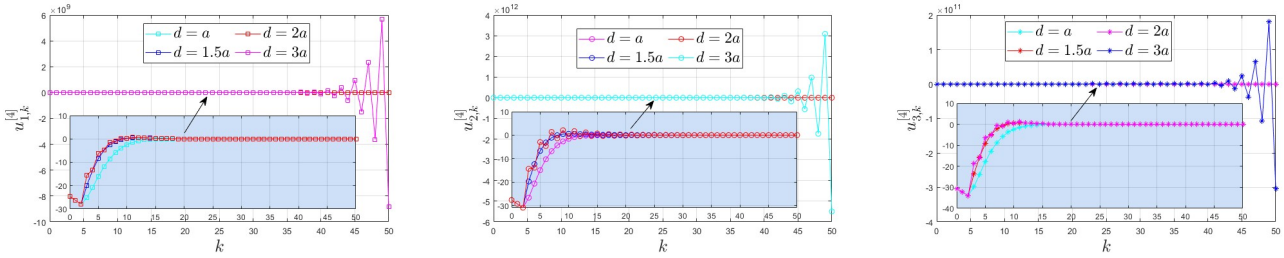

Figure 19. Exponential stabilization ($u^{[4]}_{1\to3,k}$) with different control coefficients.

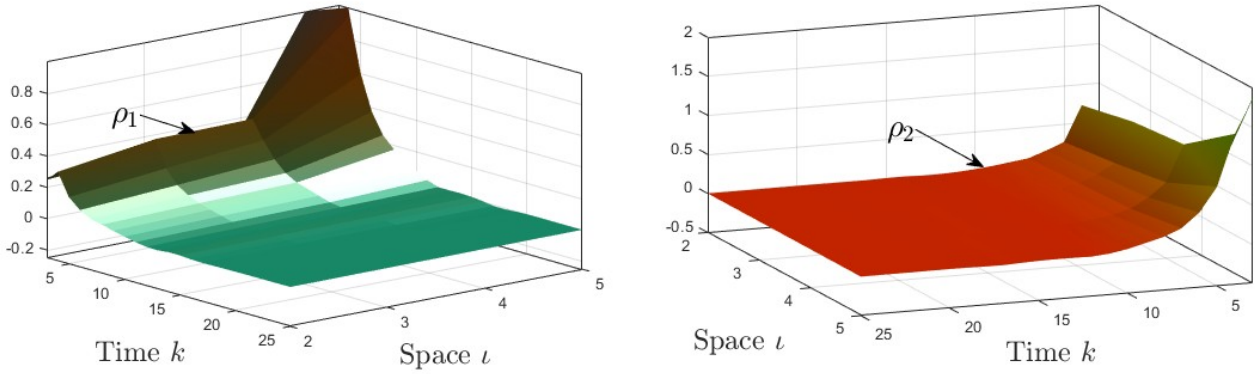

Figure 20. 3D feedback controls $\rho^{[\iota]}_{1,k}$, $\rho^{[\iota]}_{2,k}$.

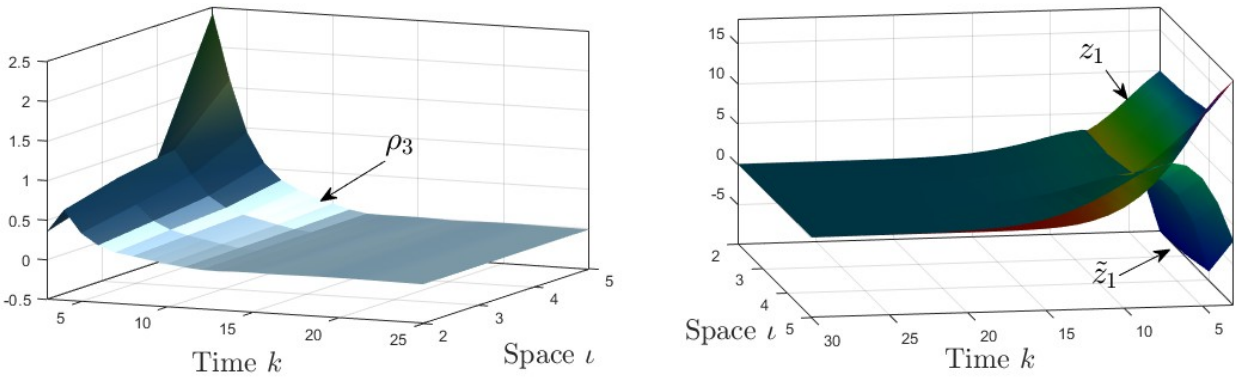

Figure 21. 3D feedback control $\rho^{[\iota]}_{3,k}$ and master-slave states $z^{[\iota]}_{1,k}$, $\tilde{z}^{[\iota]}_{1,k}$.

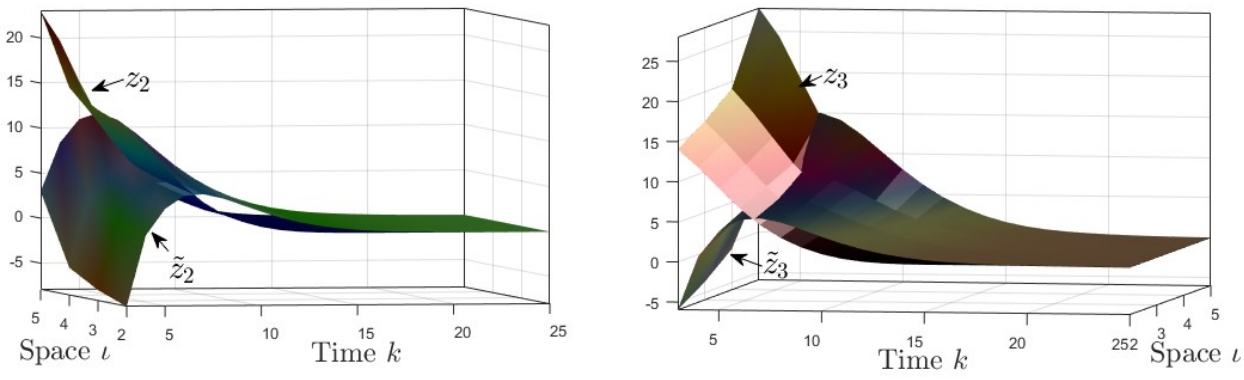

Figure 22. 3D master-slave states $z^{[\iota]}_{2\to 3,k}$.

The theoretical developments and numerical validations presented in this work offer several concrete implications for reliability engineering and safety-critical system design.

The established mean-square (μ, ν)-pseudo Weyl almost periodic sequence (MS-(μ, ν)-PWAPS) framework provides not only a mathematical criterion for stochastic stability, but also a quantitative reliability descriptor for systems operating under uncertainty. Specifically, the condition $\mathfrak{R}_* < 1$ guarantees that the probability of divergence remains bounded, serving as an intrinsic reliability margin. The exponential convergence rate can be interpreted as the system's resilience index, indicating the expected rate of recovery after random perturbations. Thus, the proposed framework bridges theoretical stochastic stability with measurable reliability indicators such as failure probability and mean time to unsafe deviation.

From an engineering viewpoint, the derived inequalities in conditions (i_7) and (i_8) provide practical guidelines for the selection of diffusion intensity, damping, and control gains. The inequality margins can be interpreted as reliability reserves, defining safe regions in parameter space where the closed-loop system maintains acceptable failure probabilities. This enables a risk-informed tuning process: increasing damping or diffusion enhances reliability at the expense of slower convergence, whereas overly aggressive control may yield fast transient response but may also involve reduced safety margins and shorter fatigue life. Such trade-offs are central to reliability-oriented control design in safety-critical mechatronic systems.

The proposed stochastic neural-network-based framework can be embedded into digital twin environments for real-time reliability monitoring, fault prediction, and safety assurance. By linking stochastic stability analysis to reliability-oriented measures, the methodology supports both predictive reliability assessment and proactive control design. This connection transforms abstract stochastic dynamics theory into a usable reliability evaluation tool for complex cyber-physical systems.

Overall, the theoretical results not only guarantee stability in a probabilistic sense but also enhance interpretability and applicability in reliability engineering contexts. They enable a unified perspective that connects mathematical rigor with engineering judgment, aligning the present study with the practical goals of risk-informed design and safe operation in stochastic environments.

Remark 5.1. *Although real robotic systems may involve more complex nonlinear and time-varying fault mechanisms, the present model captures the essential stochastic degradation characteristics while*

maintaining mathematical analyzability. The proposed framework can be extended to more general fault structures under suitable boundedness and stochastic assumptions.

6. Conclusions

This paper has developed a comprehensive theoretical and computational framework for the analysis and control of discrete-time stochastic inertial neural networks (SINNs) with communication delays and diffusion perturbations. By establishing the existence and exponential mean-square stability of (μ, ν)-pseudo Weyl almost periodic sequences (MS-(μ, ν)-PWAPSs), the work extends classical stochastic stability theory toward a reliability-oriented paradigm that is both mathematically rigorous and engineeringly interpretable.

From a theoretical perspective, the introduced MS-(μ, ν)-PWAPS concept and the derived stability criterion $\mathscr{R}^* < 1$ provide a unified description of bounded stochastic dynamics under uncertain environments. These results ensure that the system trajectories remain mean-square bounded and exhibit predictable oscillatory behavior, which corresponds to a low failure probability and stable long-term operation.

From an engineering viewpoint, the analytical conditions such as (i_7)–(i_8) and the reliability-oriented numerical simulations demonstrate how stochastic stability properties can be translated into measurable reliability indicators, including bounded failure probability, hazard rate suppression, and extended mean time to failure. The numerical experiments on the robotic joint system validate that satisfying $\mathfrak{R}_* < 1$ and (i_7)–(i_8) not only guarantees theoretical stability but also enhances operational reliability, enabling risk-informed tuning of diffusion, damping, and control parameters.

Overall, the proposed stochastic control strategy contributes a dual-layer advancement: 1) a mathematically novel treatment of stochastic inertial neural dynamics within the framework of pseudo almost periodicity; and 2) a reliability-engineering interpretation that bridges stochastic stability with practical safety and maintenance decision-making. This integration provides a new path for the design of intelligent, reliable, and resilient control systems operating under random disturbances, with potential applications in robotics, networked mechatronic systems, and cyber–physical safety architectures.

Future research will aim to extend the proposed framework to time-varying networks, adaptive event-triggered control, and hybrid reliability assessment that couples probabilistic modeling with data-driven diagnostics, further enhancing its applicability to real-world reliability engineering problems.

Use of AI tools declaration

The authors declare they have not used Artificial Intelligence (AI) tools in the creation of this article.

Acknowledgments

This work was supported by the Key Scientific Research Projects of Colleges and Universities of Henan Province under Grant No. 25B110028, the National Natural Science Foundation of China under Grant No. 62463032, the Yunnan Fundamental Research Projects under Grant No. 202501AT070209, and the Scientific Research Funds of the Educational Department of Yunnan Province under Grant No. 2024J0030.

Conflict of interest

The authors declare there is no conflict of interest.

References

1. P. Kowsalya, S. Kathiresan, A. Kashkynbayev, R. Rakkiyappan, Fixed-time synchronization of delayed multiple inertial neural network with reaction-diffusion terms under cyber-physical attacks using distributed control and its application to multi-image encryption, *Neural Netw.*, **180** (2024), 106743. https://doi.org/10.1016/j.neunet.2024.106743
2. T. Dong, R. He, H. Q. Li, W. J. Hu, T. W. Huang, Exponential stabilization of phase-change inertial neural networks with time-varying delays, *IEEE Trans. Syst. Man Cybern. Syst.*, **55** (2025), 2659–2669. https://doi.org/10.1109/TSMC.2024.3525038
3. R. Eischens, T. Li, G. W. Vogl, Y. Cai, Y. Qu, State space neural network with nonlinear physics for mechanical system modeling, *Reliab. Eng. Syst. Saf.*, **259** (2025), 110946. https://doi.org/10.1016/j.ress.2025.110946
4. J. Fernández, J. Chiachío, J. Barros, M. Chiachío, C. S. Kulkarni, Physics-guided recurrent neural network trained with approximate Bayesian computation: A case study on structural response prognostics, *Reliab. Eng. Syst. Saf.*, **243** (2024), 109822. https://doi.org/10.1016/j.ress.2023.109822
5. J. Li, Q. C. Lu, P. C. Xu, L. Liu, S. Wang, Critical station identification for cascading failure mitigation considering the Lyapunov-stability of metro stations, *Reliab. Eng. Syst. Saf.*, **256** (2025), 110772. https://doi.org/10.1016/j.ress.2024.110772
6. T. W. Zhang, Y. T. Liu, H. Z. Qu, Global mean-square exponential stability and random periodicity of discrete-time stochastic inertial neural networks with discrete spatial diffusions and Dirichlet boundary condition, *Comput. Math. Appl.*, **141** (2023), 116–128. https://doi.org/10.1016/j.camwa.2023.04.011
7. E. A. Assali, Direct approach on projective synchronization of inertial quaternion-valued neural networks with proportional delays, *Comput. Appl. Math.*, **43** (2024), 441. https://doi.org/10.1007/s40314-024-02954-6
8. L. Zhou, Q. Zhu, T. Huang, Global polynomial synchronization of proportional delayed inertial neural networks, *IEEE Trans. Syst. Man Cybern. Syst.*, **53** (2023), 4487–4497. https://doi.org/10.1109/TSMC.2023.3249664
9. K. Udhayakumar, S. Shanmugasundaram, A. Kashkynbayev, R. Rakkiyappan, Saturated and asymmetric saturated control for projective synchronization of inertial neural networks with delays and discontinuous activations through matrix measure method, *ISA Trans.*, **142** (2023), 198–213. https://doi.org/10.1016/j.isatra.2023.07.022
10. Z. X. Zhang, H. Q. Li, T. M. Li, J. X. Zhang, X. S. Si, An optimal condition-based maintenance policy for nonlinear stochastic degrading systems, *Reliab. Eng. Syst. Saf.*, **251** (2024), 110349. https://doi.org/10.1016/j.ress.2024.110349

11. N. Manoj, R. Sriraman, Global Mittag-Leffler stability and synchronization of fractional-order Clifford-valued delayed neural networks with reaction-diffusion terms and its application to image encryption, *Inf. Sci.*, **698** (2025), 121773. https://doi.org/10.1016/j.ins.2024.121773
12. T. W. Zhang, Y. Y. Yang, S. F. Han, Exponential heterogeneous anti-synchronization of multi-variable discrete stochastic inertial neural networks with adaptive corrective parameter, *Eng. Appl. Artif. Intell.*, **142** (2025), 109871. https://doi.org/10.1016/j.engappai.2024.109871
13. T. W. Zhang, H. Z. Qu, Y. T. Liu, J. W. Zhou, Weighted pseudo θ-almost periodic sequence solution and guaranteed cost control for discrete-time and discrete-space stochastic inertial neural networks, *Chaos Solitons Fractals*, **173** (2023), 113658. https://doi.org/10.1016/j.chaos.2023.113658
14. V. Gafiychuk, B. Datsko, V. Meleshko, Mathematical modeling of time fractional reaction–diffusion systems, *J. Comput. Appl. Math.*, **220** (2008), 215–225. https://doi.org/10.1016/j.cam.2007.08.011
15. K. Wang, P. P. Menon, J. Veenman, S. Bennani, Safety exploration using Gaussian process classification for uncertain systems, *Reliab. Eng. Syst. Saf.*, **256** (2025), 110680. https://doi.org/10.1016/j.ress.2024.110680
16. K. M. Mohammad, M. Kamrujjaman, Stochastic differential equations to model influenza transmission with continuous and discrete-time Markov chains, *Alexandria Eng. J.*, **110** (2025), 329–345. https://doi.org/10.1016/j.aej.2024.10.012
17. R. Oura, T. Ushio, A. Sakakibara, Bounded synthesis and reinforcement learning of supervisors for stochastic discrete event systems with LTL specifications, *IEEE Trans. Autom. Control*, **69** (2024), 6668–6683. https://doi.org/10.1109/tac.2024.3376723
18. M. Jiménez-Lizárraga, B. A. Escobedo-Trujillo, J. D. López-Barrientos, Mixed deterministic and stochastic disturbances in a discrete-time Nash game, *Int. J. Syst. Sci.*, **56** (2025), 409–422. https://doi.org/10.1080/00207721.2024.2394567
19. Y. Chen, C. D. Lu, X. M. Zhang, Allowable delay set flexible fragmentation approach to passivity analysis of delayed neural networks, *Neurocomputing*, **629** (2025), 129730. https://doi.org/10.1016/j.neucom.2025.129730
20. T. W. Zhang, H. Z. Qu, J. W. Zhou, Asymptotically almost periodic synchronization in fuzzy competitive neural networks with Caputo-Fabrizio operator, *Fuzzy Sets Syst.*, **471** (2023), 108676. https://doi.org/10.1016/j.fss.2023.108676
21. A. Hamidoglu, M. H. Taghiyev, On construction of almost periodic sequences and applications to some discrete population models, *J. Differ. Equ. Appl.*, **27** (2021), 118–131. https://doi.org/10.1080/10236198.2021.1876039
22. V. Bergelson, J. Kulaga-Przymus, M. Lemańczyk, F. K. Richter, Rationally almost periodic sequences, polynomial multiple recurrence and symbolic dynamics, *Ergodic Theory Dyn. Syst.*, **39** (2019), 2332–2383. https://doi.org/10.1017/etds.2017.130
23. W. W. Qi, Y. K. Li, Weyl almost anti-periodic solution to a neutral functional semilinear differential equation, *Electron. Res. Arch.*, **31** (2023), 1662–1672. https://doi.org/10.3934/era.2023086

24. M. Es-saiydy, M. Zitane, Dynamics analysis of delayed fuzzy Clifford-valued model: A case of Equi-Weyl almost periodic environment, *Comput. Appl. Math.*, **42** (2023), 342. https://doi.org/10.1007/s40314-023-02470-z

25. A. Arbi, N. Tahri, New results on time scales of pseudo Weyl almost periodic solution of delayed QVSICNNs, *Comput. Appl. Math.*, **41** (2022), 293. https://doi.org/10.1007/s40314-022-02003-0

26. X. M. Zhang, Q. L. Han, X. H. Ge, D. R. Ding, An overview of recent developments in Lyapunov–Krasovskii functionals and stability criteria for recurrent neural networks with time-varying delays, *Neurocomputing*, **313** (2018), 392–401. https://doi.org/10.1016/j.neucom.2018.06.038

27. T. N. S. Dongmo, J. Kengne, J. C. Chedjou, Effect of electromagnetic radiations on the dynamics of a five-chain coupled inertial Hopfield neural network and control of multi-stability with the selection of a desired attractor, *Phys. Scr.*, **100** (2025), 015013. https://doi.org/10.1088/1402-4896/ad8e95

28. Y. X. Jiang, S. Zhu, X. Y. Liu, S. P. Wen, C. X. Mu, Input-to-state stability of delayed memristor-based inertial neural networks via non-reduced order method, *Neural Netw.*, **178** (2024), 106545. https://doi.org/10.1016/j.neunet.2024.106545

29. S. Singh, U. Kumar, S. Das, J. D. Cao, Global exponential stability of inertial Cohen-Grossberg neural networks with time-varying delays via feedback and adaptive control schemes: Non-reduction order approach, *Neural Process. Lett.*, **55** (2023), 4347–4363. https://doi.org/10.1007/s11063-022-11044-9

30. H. C. Lin, H. B. Zeng, X. M. Zhang, W. Wang, Stability analysis for delayed neural networks via a generalized reciprocally convex inequality, *IEEE Trans. Neural Netw. Learn. Syst.*, **34** (2023), 7491–7499. https://doi.org/10.1109/TNNLS.2022.3144032

31. H. Liang, J. Xie, B. Huang, Y. Li, B. Sun, C. Yang, A novel sim2real reinforcement learning algorithm for process control, *Reliab. Eng. Syst. Saf.*, **254** (2025), 110639. https://doi.org/10.1016/j.ress.2024.110639

32. G. D. Zhang, J. D. Cao, Aperiodically semi-intermittent-based fixed-time stabilization and synchronization of delayed discontinuous inertial neural networks, *Sci. China Inf. Sci.*, **68** (2025), 112202. https://doi.org/10.1007/s11432-023-4053-9

33. Y. Y. Zhang, F. C. Kong, Q. X. Zhu, T. W. Huang, Quantized control based on stabilization of discontinuous memristor-based fuzzy inertial neural networks with proportional delays, *IEEE Trans. Syst. Man Cybern. Syst.*, **54** (2024), 5756–5767. https://doi.org/10.1109/tsmc.2024.3408469

34. S. Y. Jia, L. Q. Zhou, Fixed-time stabilization of fuzzy neutral-type inertial neural networks with proportional delays, *ISA Trans.*, **144** (2024), 167–175. https://doi.org/10.1016/j.isatra.2023.10.032

35. R. N. Guo, Y. Z. Zhu, C. K. Ahn, Non-reduced order method to parameterized sampled-data stabilization of inertial neural networks with actuator saturation, *IEEE Trans. Circuits Syst. I Regul. Pap.*, **72** (2025), 2288–2301. https://doi.org/10.1109/tcsi.2024.3511041

36. M. Q. Shen, C. Wang, Q. G. Wang, Y. H. Sun, G. D. Zong, Synchronization of fractional reaction–diffusion complex networks with unknown couplings, *IEEE Trans. Netw. Sci. Eng.*, **11** (2024), 4503–4512. https://doi.org/10.1109/TNSE.2024.3432997

37. M. Q. Shen, C. Wang, Q. G. Wang, H. C. Yan, G. D. Zong, Z. H. Zhu, Fault-tolerant synchronization control of switched complex networks by a proportional-integral intermediate observer approach, *IEEE Trans. Cybern.*, **55** (2025), 4689–4698. https://doi.org/10.1109/TCYB.2025.3591393

38. D. Roy, G. V. Rao, *Stochastic Dynamics, Filtering and Optimization*, Cambridge University Press, Cambridge, 2017. https://doi.org/10.1017/9781316863107

39. M. Engel, *Lecture Notes on Random Dynamical Systems*, FU Berlin, 2021.

40. A. Rebey, H. Ben-Elmonser, M. Eljeri, M. Miraoui, Pseudo-almost periodic solutions in the Alpha-norm and in Stepanov's sense for some evolution equations, *Ukr. Math. J.*, **74** (2022), 1599–1616. https://doi.org/10.37863/umzh.v74i10.6315

41. P. Raynaud de Fitte, Almost periodicity and periodicity for nonautonomous random dynamical systems, *Stoch. Dyn.*, **21** (2020), 2150034. https://doi.org/10.1142/s0219493721500349

42. Y. K. Li, X. Huang, X. Wang, Weyl almost periodic solutions for quaternion-valued shunting inhibitory cellular neural networks with time-varying delays, *AIMS Math.*, **7** (2021), 4861–4886. https://doi.org/10.3934/math.2022271

43. Z. Z. Sun, Q Zhang, G Gao, *Finite Difference Method for Nonlinear Evolution Equations*, Science Press, Beijing, 2023.

44. X. L. Hao, Z. Q. Ge, *Optimization and Optimal Control* (in Chinese), Xi'an Jiaotong University Press, Xi'an, 2015.

45. D. O'Regan, Y. J. Cho, Y. Q. Chen, *Topological Degree Theory and Applications*, Taylor & Francis, Boca Raton, 2006. https://doi.org/10.1201/9781420011487

46. C. Y. Wang, Z. G. Yang, *Delay Peaction–Diffusion Equation and Upper and Lower Solution Method* (in Chinese), Science Press, Beijing, 2013.

Appendix

A. Proof of the propositions

Proof of Proposition 3.1. By the definition of $\mathbb{ERG}(\mathbb{Z}, \mathbb{L}^2(\mathbb{P}, \mathbb{R}), \mu, \nu)$, we have

$$\begin{aligned}\frac{1}{\nu([-\ell,\ell]_{\mathbb{Z}})}\sum_{s=-\ell}^{\ell-1}\|z_{s-\delta_s}\|_2\mu([s,s+1]_{\mathbb{Z}}) \le{}& \frac{1}{\nu([-\ell,\ell]_{\mathbb{Z}})}\sum_{s=-\ell}^{\ell-1}\|z_s\|_2\mu([s,s+1]_{\mathbb{Z}})\frac{\mu([s,s+\delta_\infty+1]_{\mathbb{Z}})}{\mu([s,s+1]_{\mathbb{Z}})}\\ &+\frac{1}{\nu([-\ell,\ell]_{\mathbb{Z}})}\sum_{s=-\ell-\delta_\infty}^{-\ell-1}\|z_s\|_2\mu([s,s+\delta_\infty+1]_{\mathbb{Z}})\\ \le{}& \frac{\varkappa_1(\delta_\infty+1)}{\varkappa_0}\frac{1}{\nu([-\ell,\ell]_{\mathbb{Z}})}\sum_{s=-\ell}^{\ell-1}\|z_s\|_2\mu([s,s+1]_{\mathbb{Z}})\\ &+\frac{\varkappa_1(\delta_\infty+1)}{\nu([-\ell,\ell]_{\mathbb{Z}})}\sum_{s=-\ell-\delta_\infty}^{-\ell-1}\|z_s\|_2\to 0,\ \text{as}\ \ell\longrightarrow+\infty.\end{aligned}$$

Thus, $z_{k-\delta_k}\in\mathbb{ERG}(\mathbb{Z},\mathbb{R},\mu,\nu)$, $\forall k\in\mathbb{Z}$. This completes the proof.

Proof of Proposition 3.2. Supposing $\tau \in \mathbb{Z}$ is the ϵ-almost period of δ and z, then $\|\mathfrak{T}_\tau z_{k-\delta_k} - z_{k-\delta_k}\|_2 \leq \|\mathfrak{T}_\tau z_{k-\delta_k} - z_{k-\delta_{k+\tau}}\|_2 + \|z_{k-\delta_{k+\tau}} - z_{k-\delta_k}\|_2 = \|\mathfrak{T}_\tau z_{k-\delta_k} - z_{k-\delta_{k+\tau}}\|_2, \forall k \in \mathbb{Z}$, which induces that

$$\begin{aligned}
\|\mathfrak{T}_\tau z_{k-\delta_k} - z_{k-\delta_k}\|_{\mathbb{W}^2} &\leq \lim_{K\to+\infty} \sup_{k\in\mathbb{Z}} \Big[\frac{1}{K} \sum_{s=k}^{k+K-1} \sum_{l=0}^{\delta_\infty} \|z_{s-l+\tau} - z_{s-l}\|_2^2\Big]^{\frac{1}{2}} \\
&\overset{s'=s-l}{=\!=} \lim_{K\to+\infty} \sup_{k\in\mathbb{Z}} \Big[\frac{1}{K} \sum_{l=0}^{\delta_\infty} \sum_{s'=k-l}^{k-l+K-1} \|z_{s'+\tau} - z_{s'}\|_2^2\Big]^{\frac{1}{2}} \\
&\leq \sum_{l=0}^{\delta_\infty} \lim_{K\to+\infty} \sup_{(k-l)\in\mathbb{Z}} \Big[\frac{1}{K} \sum_{s'=k-l}^{k-l+K-1} \|z_{s'+\tau} - z_{s'}\|_2^2\Big]^{\frac{1}{2}} \\
&\overset{k'=k-l}{=\!=} \sum_{l=0}^{\delta_\infty} \lim_{K\to+\infty} \sup_{k'\in\mathbb{Z}} \Big[\frac{1}{K} \sum_{s'=k'}^{k'+K-1} \|z_{s'+\tau} - z_{s'}\|_2^2\Big]^{\frac{1}{2}}.
\end{aligned}$$

So $z_{k-\delta_k} \in \mathbb{W}^2\mathbb{AP}^\vartheta(\mathbb{Z}, \mathbb{L}^2(\mathbb{P}, \mathbb{R}))$ owing to $z_k \in \mathbb{W}^2\mathbb{AP}^\vartheta(\mathbb{Z}, \mathbb{L}^2(\mathbb{P}, \mathbb{R}))$, $\forall k \in \mathbb{Z}$. This completes the proof.

Proof of Proposition 3.4. Since $b \in \mathbb{W}^2\mathbb{PAP}(\mathbb{Z}, \mathbb{R}), \mu, \nu)$ and $z \in \mathbb{W}^2\mathbb{PAP}^\vartheta(\mathbb{Z}, \mathbb{L}^2(\mathbb{P}, \mathbb{R}), \mu, \nu)$, then $b = \hat{b} + \check{b}, z = \hat{z} + \check{z}$, where $\hat{b} \in \mathbb{W}^2\mathbb{AP}(\mathbb{Z}, \mathbb{R})$, $\hat{z} \in \mathbb{W}^2\mathbb{AP}^\vartheta(\mathbb{Z}, \mathbb{L}^2(\mathbb{P}, \mathbb{R}))$, $\check{b} \in \mathbb{ERG}(\mathbb{Z}, \mathbb{R}, \mu, \nu)$, and $\check{z} \in \mathbb{ERG}(\mathbb{Z}, \mathbb{L}^2(\mathbb{P}, \mathbb{R}), \mu, \nu)$. By the boundedness of $z, \check{z}, b, \check{b}$, there exist some positive constants $\check{z}_0, \check{b}_0, \hat{z}_0, \hat{b}_0$ such that $\|\check{z}\|_\infty \leq \check{z}_0, \|\check{b}\|_\infty \leq \check{b}_0, \|\hat{z}\|_\infty \leq \hat{z}_0, \|\hat{b}\|_\infty \leq \hat{b}_0$.

For any $\tau \in \mathbb{Z}$, we have

$$\begin{aligned}
\|\mathfrak{T}_\tau \hat{b}_k f(\hat{z}_k) - \hat{b}_k f(\hat{z}_k)\|_{\mathbb{W}^2} &= \|\hat{b}_{k+\tau} f(\mathfrak{T}_\tau \hat{z}_k) - \hat{b}_k f(\hat{z}_k)\|_{\mathbb{W}^2} \\
&\leq \|\hat{b}_{k+\tau} - \hat{b}_k\|_{\mathbb{W}^2} |L_f \hat{z}_0 + \hat{b}_0 L_f| \|\mathfrak{T}_\tau \hat{z}_k - \hat{z}_k\|_{\mathbb{W}^2}, \quad \forall k \in \mathbb{Z},
\end{aligned}$$

which implies $\hat{b} f(\hat{z}) \in \mathbb{W}^2\mathbb{AP}^\vartheta(\mathbb{Z}, \mathbb{L}^2(\mathbb{P}, \mathbb{R}))$. Meanwhile, $|bf(z) - \hat{b} f(\hat{z})| \leq |\check{b}||f(z)| + |\hat{b}|L_f|\check{z}| \leq L_f z_0 |\check{b}| + \hat{b}_0 L_f |\check{z}|$, which induces $bf(z) - \hat{b} f(\hat{z}) \in \mathbb{ERG}(\mathbb{Z}, \mathbb{L}^2(\mathbb{P}, \mathbb{R}), \mu, \nu)$. Since $bf(z) = \hat{b} f(\hat{z}) + bf(z) - \hat{b} f(\hat{z})$, we obtain $bf(z) \in \mathbb{W}^2\mathbb{PAP}^\vartheta(\mathbb{Z}, \mathbb{L}^2(\mathbb{P}, \mathbb{R}), \mu, \nu)$. This completes the proof.

Proof of Proposition 3.5. Since $z_j \in \mathbb{W}^2\mathbb{PAP}^\vartheta(\mathbb{Z}, \mathbb{L}^2(\mathbb{P}, \mathbb{R}), \mu, \nu)$, then $z_j = \hat{z}_j + \check{z}_j$, where $\hat{z}_j \in \mathbb{W}^2\mathbb{AP}^\vartheta(\mathbb{Z}, \mathbb{L}^2(\mathbb{P}, \mathbb{R}))$, $\check{z}_j \in \mathbb{ERG}(\mathbb{Z}, \mathbb{L}^2(\mathbb{P}, \mathbb{R}), \mu, \nu)$, $j = 1, 2, \ldots, n$. Define $\hat{\Gamma}_{j,k} = \sum_{l=1}^\infty \sigma_{jl}(\hat{z}_{j,k}) \varepsilon_{l,k}, \check{\Gamma}_{j,k} = \sum_{l=1}^\infty \Big[\sigma_{jl}(z_{j,k}) - \sigma_{jl}(\check{z}_{j,k})\Big] \varepsilon_{l,k}, \forall k \in \mathbb{Z}$. For any $\tau \in \mathbb{Z}$, we have

$$\|\mathfrak{T}_\tau \hat{\Gamma}_{j,k} - \hat{\Gamma}_{j,k}\|_2^2 \leq \mathbf{E}\Big[\sum_{l=1}^\infty L_{jl}^\sigma \Big|\mathfrak{T}_\tau \hat{z}_{j,k} - \hat{z}_{j,k}\Big| |\varepsilon_{l,k}|\Big]^2 \leq (L_{j*}^\sigma)^2 \mathbf{E}|\mathfrak{T}_\tau \hat{z}_{j,k} - \hat{z}_{j,k}|^2,$$

which induces

$$\|\mathfrak{T}_\tau \hat{\Gamma}_j - \hat{\Gamma}_j\|_{\mathbb{W}^2} \leq (L_{j*}^\sigma)^2 \lim_{K\to+\infty} \sup_{k\in\mathbb{Z}} \Big[\frac{1}{K} \sum_{s=k}^{k+K-1} \mathbf{E}|\mathfrak{T}_\tau \hat{z}_{j,k} - \hat{z}_{j,k}|_2^2\Big]^{\frac{1}{2}} = (L_{j*}^\sigma)^2 \|\mathfrak{T}_\tau \hat{z}_{j,k} - \hat{z}_{j,k}\|_{\mathbb{W}^2},$$

so $\hat{\Gamma}_j \in \mathbb{W}^2\mathbb{AP}^\vartheta(\mathbb{Z}, \mathbb{L}^2(\mathbb{P}, \mathbb{R}))$ for $j = 1, 2, \ldots, n$.

Next, it suffices to prove $\check{\Gamma}_j \in \mathbb{ERG}(\mathbb{Z}, \mathbb{L}^2(\mathbb{P}, \mathbb{R}), \mu, \nu)$ for $j = 1, 2, \ldots, n$. In fact, $\|\check{\Gamma}_{j,k}\|_2^2 \leq \mathbf{E}\Big[\sum_{l=1}^\infty L_{jl}^\sigma |\check{z}_{j,k}| \|\varepsilon_{l,k}|\Big]^2 \leq (L_{j*}^\sigma)^2 \mathbf{E}|\check{z}_{j,k}|^2$, which induces $\check{\Gamma}_j \in \mathbb{ERG}(\mathbb{Z}, \mathbb{L}^2(\mathbb{P}, \mathbb{R}), \mu, \nu)$, $j = 1, 2, \ldots, n$. This completes the proof.

Proof of Proposition 3.6. Via Lemma 2.1, we have

$$\begin{aligned}\|\mathfrak{T}_\tau\hat{\Lambda}_k-\hat{\Lambda}_k\|_2^2 &\le \sum_{q=-\infty}^{k-1}\sum_{s=-\infty}^{q-1} e^{-a(k-s-2)h}\times\sum_{q=-\infty}^{k-1}\sum_{s=-\infty}^{q-1} e^{-a(k-s-2)h}\mathbf{E}(\mathfrak{T}_\tau\hat{z}_s-\hat{z}_s)^2\\ &\le \frac{1}{(1-e^{-ah})^2}\sum_{q=-\infty}^{-1}\sum_{s=-\infty}^{-1} e^{a(q+s+2)h}\|\mathfrak{T}_\tau\hat{z}_{k+q+s}-\hat{z}_{k+q+s}\|_2^2,\end{aligned}$$

which implies

$$\begin{aligned}\|\mathfrak{T}_\tau\hat{\Lambda}-\hat{\Lambda}\|_{\mathbb{W}^2} &\le \frac{1}{1-e^{-ah}}\lim_{K\to+\infty}\sup_{k\in\mathbb{Z}}\Big[\frac{1}{K}\sum_{s'=k}^{k+K-1}\sum_{q=-\infty}^{-1}\sum_{s=-\infty}^{-1} e^{a(q+s+2)h}\|\mathfrak{T}_\tau\hat{z}_{s'+q+s}-\hat{z}_{s'+q+s}\|_2^2\Big]^{\frac{1}{2}}\\ &\le \frac{1}{1-e^{-ah}}\lim_{K\to+\infty}\Big[\sum_{q=-\infty}^{-1}\sum_{s=-\infty}^{-1} e^{a(q+s+2)h}\sup_{k\in\mathbb{Z}}\frac{1}{K}\sum_{s''=k+q+s}^{k+q+s+K-1}\|\mathfrak{T}_\tau\hat{z}_{s''}-\hat{z}_{s''}\|_2^2\Big]^{\frac{1}{2}}\\ &\le \frac{1}{1-e^{-ah}}\Big[\sum_{q=-\infty}^{-1}\sum_{s=-\infty}^{-1} e^{a(q+s+2)h}\lim_{K\to+\infty}\sup_{k'\in\mathbb{Z}}\frac{1}{K}\sum_{s''=k'}^{k'+K-1}\|\mathfrak{T}_\tau\hat{z}_{s''}-\hat{z}_{s''}\|_2^2\Big]^{\frac{1}{2}}\\ &\le \frac{1}{1-e^{-ah}}\Big[\sum_{q=-\infty}^{-1}\sum_{s=-\infty}^{-1} e^{a(q+s+2)h}\Big]^{\frac{1}{2}}\|\mathfrak{T}_\tau\hat{z}-\hat{z}\|_{\mathbb{W}^2}\le\frac{1}{(1-e^{-ah})^2}\|\mathfrak{T}_\tau\hat{z}-\hat{z}\|_{\mathbb{W}^2}.\end{aligned}$$

So $\hat{\Lambda}\in\mathbb{W}^2\mathbb{AP}^\vartheta(\mathbb{Z},\mathbb{L}^2(\mathbb{P},\mathbb{R}))$. This completes the proof.

Proof of Proposition 3.7. Define $\check{\Lambda}_k^r=\sum_{q=k-r-2}^{k-r-1}\sum_{s=-\infty}^{q-1}e^{-a(k-s-2)h}\check{z}_s$, $\forall k\in\mathbb{Z}, r=0,1,\ldots$. By Lemma 2.1, we get

$$\sum_{r=0}^{+\infty}\|\check{\Lambda}_k^r\|_2\le\sum_{r=0}^{+\infty}\Big[\sum_{q=k-r-2}^{k-r-1}\sum_{s=-\infty}^{q-1}e^{-a(k-s-2)h}\sum_{q=k-r-2}^{k-r-1}\sum_{s=-\infty}^{q-1}e^{-a(k-s-2)h}\|\check{z}_s\|_2^2\Big]^{\frac{1}{2}}\le\frac{\|\check{z}\|_\infty^2}{(1-e^{-ah})^2}<\infty,\quad\forall k\in\mathbb{Z},$$

which induces that $\|\check{\Lambda}_k\|_2\le\sum_{r=0}^{+\infty}\|\check{\Lambda}_k^r\|_2\le\frac{\|\check{z}\|_\infty^2}{(1-e^{-ah})^2}<\infty$, $\forall k\in\mathbb{Z}$. Then $\check{\Lambda}_k=\sum_{r=0}^{+\infty}\check{\Lambda}_k^r$ is uniformly convergent on $k\in\mathbb{Z}$. That is, for any $\epsilon>0$, there exists $r'\in\mathbb{Z}_+$ such that, for $r_0>r'$, $\sup_{k\in\mathbb{Z}}\Big\|\check{\Lambda}_k-\sum_{r=0}^{r_0}\check{\Lambda}_k^r\Big\|_2<\epsilon$.

Define $\check{\Lambda}_k^{r_0,r}=\sum_{q=k-r_0-2}^{k-1}\sum_{s=q-r-2}^{q-r-1}e^{-a(k-s-2)h}\check{z}_s$, $\forall k\in\mathbb{Z}, r=0,1,\ldots$. Similarly,

$$\sum_{r=0}^{+\infty}\|\check{\Lambda}_k^{r_0,r}\|_2\le\sum_{r=0}^{+\infty}\Big[\sum_{q=k-r_0-2}^{k-1}\sum_{s=q-r-2}^{q-r-1}e^{-a(k-s-2)h}\sum_{q=k-r_0-2}^{k-1}\sum_{s=q-r-2}^{q-r-1}e^{-a(k-s-2)h}\|\check{z}_s\|_2^2\Big]^{\frac{1}{2}}\le\frac{\|\check{z}\|_\infty^2}{(1-e^{-ah})^2}<\infty,$$

so $\sum_{r=0}^{r_0}\check{\Lambda}_k^r=\sum_{r=0}^{+\infty}\check{\Lambda}_k^{r_0,r}$ is uniformly convergent on $k\in\mathbb{Z}$. That is, there exists $r''\in\mathbb{Z}_+$ so that, for $r_1>r''$, $\sup_{k\in\mathbb{Z}}\Big\|\sum_{r=0}^{r_0}\check{\Lambda}_k^r-\sum_{r=0}^{r_1}\check{\Lambda}_k^{r_0,r}\Big\|_2<\epsilon$.

Moreover,

$$\begin{aligned}\sum_{r=0}^{r_1}\check{\Lambda}_k^{r_0,r}=&(\check{z}_{k-2}+e^{-ah}\check{z}_{k-3}+\cdots+e^{-a(r_1+1)h}\check{z}_{k-r_1-3})\\ &+(e^{-ah}\check{z}_{k-3}+e^{-2ah}\check{z}_{k-4}+\cdots+e^{-a(r_1+2)h}\check{z}_{k-r_1-4})\\ &+\cdots+(e^{-a(r_0+1)h}\check{z}_{k-r_0-3}+e^{-a(r_0+2)h}\check{z}_{k-r_0-4}+\cdots+e^{-a(r_0+r_1+2)h}\check{z}_{k-r_0-r_1-4}),\end{aligned}$$

which implies from Definition 2.1 that $\sum_{r=0}^{r_1}\check{\Lambda}_k^{r_0,r} \in \mathbb{ERG}(\mathbb{Z},\mathbb{L}^2(\mathbb{P},\mathbb{R}),\mu,\nu)$, $\forall k \in \mathbb{Z}$. In line with Definition 2.1, we have

$$\begin{aligned}
&\frac{1}{\nu([-\ell,\ell]_{\mathbb{Z}})}\sum_{s=-\ell}^{\ell-1}\|\check{\Lambda}_s\|_2\mu([s,s+1]_{\mathbb{Z}})\\
\leq\ &\frac{1}{\nu([-\ell,\ell]_{\mathbb{Z}})}\sum_{s=-\ell}^{\ell-1}\Big\|\check{\Lambda}_s-\sum_{r=0}^{r_0}\check{\Lambda}_s^{r}\Big\|_2\mu([s,s+1]_{\mathbb{Z}})\\
&+\frac{1}{\nu([-\ell,\ell]_{\mathbb{Z}})}\sum_{s=-\ell}^{\ell-1}\Big\|\sum_{r=0}^{r_0}\check{\Lambda}_s^{r}-\sum_{r=0}^{r_1}\check{\Lambda}_s^{r_0,r}\Big\|_2\mu([s,s+1]_{\mathbb{Z}})+\frac{1}{\nu([-\ell,\ell]_{\mathbb{Z}})}\sum_{s=-\ell}^{\ell-1}\Big\|\sum_{r=0}^{r_1}\check{\Lambda}_s^{r_0,r}\Big\|_2\mu([s,s+1]_{\mathbb{Z}})\\
\leq\ &\frac{2\varkappa_1}{\varkappa_0}\epsilon+\frac{1}{\nu([-\ell,\ell]_{\mathbb{Z}})}\sum_{s=-\ell}^{\ell-1}\Big\|\sum_{r=0}^{r_1}\check{\Lambda}_s^{r_0,r}\Big\|_2\mu([s,s+1]_{\mathbb{Z}})\to\frac{2\varkappa_1}{\varkappa_0}\epsilon,\ \text{as}\ \ell\to+\infty.
\end{aligned}$$

Taking $\epsilon\to 0$, we derive the conclusion of this lemma. This completes the proof.

B. Proof of the theorems

Proof of Theorem 3.1. By Propositions 3.3-3.8, Φ maps $\mathbb{W}^2\mathbb{PAP}^{\vartheta}(\mathbb{Z}\times[0,\aleph]_{\mathbb{Z}},\mathbb{L}^2(\mathbb{P},\mathbb{R}^n),\mu,\nu)$ into itself. Define $\mathscr{D}_*=\Big\{\mathbf{z}\in\mathbb{W}^2\mathbb{PAP}^{\vartheta}(\mathbb{Z}\times[0,\aleph]_{\mathbb{Z}},\mathbb{L}^2(\mathbb{P},\mathbb{R}^n),\mu,\nu):\mathbf{z}_{\cdot}^{[0]}=0=\mathbf{z}_{\cdot}^{[\aleph]},\|\mathbf{z}\|_\infty<\mathfrak{R}_0\Big\}$, where $\mathfrak{R}_0>\max_{1\leq i\leq n}\frac{4\bar{I}_i}{(1-\mathfrak{R}_*)a_i^2}$.

Based on Eq (3.1), item 1) of Lemma 2.2, and condition (i_5) in turn, we have

$$\begin{aligned}
\|(\Phi\mathbf{z})_k\|_*\leq&\max_{1\leq i\leq n}\max_{\iota\in[0,\aleph]_{\mathbb{Z}}}\alpha_i^2\Big\|\sum_{q=-\infty}^{k-1}\sum_{\zeta=-\infty}^{q-1}e^{-\frac{1}{2}a_i(k-\zeta-2)h}\Big[\gamma_i\Delta_\iota^2 z_{i,\zeta}^{[\iota]}+\Big(\frac{1}{4}a_i^2-b_{i,\zeta}\Big)z_{i,\zeta}^{[\iota]}\\
&+\sum_{j=1}^{n}c_{ij,\zeta}f_j(z_{j,\zeta-\delta_{j,\zeta}}^{[\iota]})+\frac{1}{\sqrt{h}}\sum_{j=1}^{n}\xi_{ij,\zeta}\sum_{l=1}^{\infty}\sigma_{jl}(z_{j,\zeta-o_{j,\zeta}}^{[\iota]})\varepsilon_{l,\zeta}+I_{i,\zeta}\Big]\Big\|_2\\
\leq&\max_{1\leq i\leq n}\Big\{\frac{4}{a_i^2}\Big[\frac{4|\gamma_i|}{\hbar^2}+\bar{b}_i+\sum_{j=1}^{n}\bar{c}_{ij}L_j^f+\frac{1}{\sqrt{h}}\sum_{j=1}^{n}\bar{\xi}_{ij}L_{j*}^{\sigma}\Big]\mathfrak{R}_0+\frac{4\bar{I}_i}{a_i^2}\Big\}\leq\mathfrak{R}_*\mathfrak{R}_0+\max_{1\leq i\leq n}\frac{4\bar{I}_i}{a_i^2}<\mathfrak{R}_0,\quad\text{(B.1)}
\end{aligned}$$

$\forall k\in\mathbb{Z}$. When $\mathbf{z}\in\partial\mathscr{D}_*$, then $\|\mathbf{z}\|_\infty=\mathfrak{R}_0$ and by (B.1), $\|\Phi\mathbf{z}\|_\infty<\mathfrak{R}_0=\|\mathbf{z}\|_\infty$. Define a homotopic mapping by $H_t(\mathbf{z})=t\Phi\mathbf{z}$, $\forall t\in[0,1],\mathbf{z}\in\mathscr{D}_*$. In line with the diagonal rule in [46, page 81], $\Phi\mathbf{z}$ and $H_t(\mathbf{z})$ are continuous and compact. Next, we claim that $H_t(\mathbf{z})\neq\mathbf{z}$ for all $(t,\mathbf{z})\in[0,1]\times\partial\mathscr{D}_*$. In fact, if there exist some $\mathbf{z}\in\partial\mathscr{D}_*$ such that $H_t(\mathbf{z})=\mathbf{z}$, then $\mathbf{z}=t\Phi\mathbf{z}\Rightarrow\|\mathbf{z}\|_\infty=t\|\Phi\mathbf{z}\|_\infty\leq\|\Phi\mathbf{z}\|_\infty,\forall t\in[0,1]$. This induces a conflict. So $H_t(\mathbf{z})=t\Phi\mathbf{z}$, $\forall t\in[0,1],\mathbf{z}\in\mathscr{D}_*$. According to the homotopy of the Leray Schauder degree in Lemma 3.1, we have $1=\deg(I-H_0(\mathbf{z}),\mathscr{D}_*,0)=\deg(I-H_1(\mathbf{z}),\mathscr{D}_*,0)=\deg(I-\Phi,\mathscr{D}_*,0)$. By the solvability in Lemma 3.1, there exists a fixed point $\tilde{\mathbf{z}}\in\mathscr{D}_*$ such that $\Phi\tilde{\mathbf{z}}=\tilde{\mathbf{z}}$, which is the mean-squared (μ,ν)-pseudo WAPS of SINN (2.1). The proof is complete.

Proof of Theorem 3.2. Assume that $\bar{\mathbf{z}}=(\bar{z}_1,\bar{z}_2,\ldots,\bar{z}_n)^T$ is the another mean-squared (μ,ν)-pseudo WAPS of SINN (2.1) with the initial values (3.2). Define $\hat{\mathbf{z}}=(\hat{z}_1,\hat{z}_2,\ldots,\hat{z}_n)^T$, where $\hat{z}_i=\tilde{z}_i-\bar{z}_i$ for $i=1,2,\ldots,n$. Through item 2) of Lemma 2.2, we have

$$\|\hat{\mathbf{z}}_{i,k}^{[\iota]}\|_2^2 \le \alpha_i^4 \Big\| \sum_{q=0}^{k-1}\sum_{\zeta=0}^{q-1} e^{-\frac{1}{2}a_i(k-\zeta-2)h}\Big[\gamma_i\Delta_\iota^2\hat{z}_{i,\zeta}^{[\iota]} + \Big(\frac{1}{4}a_i^2 - b_{i,\zeta}\Big)\hat{z}_{i,\zeta}^{[\iota]}$$
$$+ \sum_{j=1}^{n} c_{ij,\zeta}(f_j(\tilde{z}_{j,\zeta-\delta_{j,\zeta}}^{[\iota]}) - f_j(\bar{z}_{j,\zeta-\delta_{j,\zeta}}^{[\iota]})) + \frac{1}{\sqrt{h}}\sum_{j=1}^{n}\xi_{ij,\zeta}\sum_{l=1}^{\infty}(\sigma_{jl}(\tilde{z}_{j,\zeta-o_{j,\zeta}}^{[\iota]}) - \sigma_{jl}(\bar{z}_{j,\zeta-o_{j,\zeta}}^{[\iota]}))\varepsilon_{l,\zeta}\Big]\Big\|_2^2$$
$$\le \frac{2(1+\delta_\infty)e^{\frac{1}{2}a_ih\delta_\infty}\alpha_i^4}{\epsilon h(1-e^{-\frac{1}{2}a_ih})^2}\sum_{\zeta=-\delta_\infty}^{k-1} e^{-(\frac{1}{2}a_i-\epsilon)(k-\zeta-2)h}\Big[\frac{4|\gamma_i|}{\hbar^2} + \bar{b}_i + \sum_{j=1}^{n}\bar{c}_{ij}L_j^f + \frac{1}{\sqrt{h}}\sum_{j=1}^{n}\bar{\xi}_{ij}L_{j*}^{\sigma}\Big]^2\|\hat{\mathbf{z}}_\zeta\|_*^2,$$

which implies $e^{(\frac{1}{2}a_*-\epsilon)kh}\|\hat{\mathbf{z}}_k\|_*^2 \le F\sum_{\zeta=-\delta_\infty}^{k-1} e^{(\frac{1}{2}a_*-\epsilon)\zeta h}\|\hat{\mathbf{z}}_\zeta\|_*^2$, $\forall k \in \mathbb{Z}_0$, where $0 < \epsilon < \min\{\frac{1}{2}a_*, \frac{1}{h}\}$ and

$$F = \max_{1\le i\le n}\frac{2(1+\delta_\infty)e^{\frac{1}{2}a_ih\delta_\infty}e^{2(\frac{1}{2}a_i-\epsilon)h}\alpha_i^4}{\epsilon h(1-e^{-\frac{1}{2}a_ih})^2}\Big[\frac{4|\gamma_i|}{\hbar^2} + \bar{b}_i + \sum_{j=1}^{n}\bar{c}_{ij}L_j^f + \frac{1}{\sqrt{h}}\sum_{j=1}^{n}\bar{\xi}_{ij}L_{j*}^{\sigma}\Big]^2.$$

Via the discrete Gronwall inequality (see Lemma 2.3), $\|\hat{\mathbf{z}}_k\|_* = 0$, $\forall k \in \mathbb{Z}_0$. This completes the proof.

Proof of Theorem 4.1. Through the first equation of Eq (4.5), and Lemma 2.4, it follows that

$$x_{i,k}^{[\iota]} = e^{-\frac{1}{2}\eta_ikh}x_{i,0}^{[\iota]} + \alpha_i\sum_{q=0}^{k-1}e^{-\frac{1}{2}\eta_i(k-q-1)h}y_{i,q}^{[\iota]}, \quad \forall(\iota,k)\in(0,\aleph)_{\mathbb{Z}}\times\mathbb{Z}_0, \tag{B.2}$$

where $i = 1, 2, \ldots, n$. Similarly,

$$y_{i,k}^{[\iota]} = e^{-\frac{1}{2}\mathscr{A}_ikh}y_{i,0}^{[\iota]} + \alpha_i\sum_{q=0}^{k-1}e^{-\frac{1}{2}\mathscr{A}_i(k-q-1)h}\Big\{\gamma_i\Delta_\iota^2x_{i,q}^{[\iota]} + (\frac{\kappa_ia_i^2}{4} - b_{i,q})x_{i,q}^{[\iota]} + \sum_{j=1}^{n}c_{ij,q}\Big[f_j(z_{j,q-\delta_{j,q}}^{[\iota]})$$
$$- f_j(\tilde{z}_{j,q-\delta_{j,q}}^{[\iota]})\Big] + \frac{1}{\sqrt{h}}\sum_{j=1}^{n}\xi_{ij,q}\sum_{l=1}^{\infty}\Big[\sigma_{jl}(z_{j,q-o_{j,q}}^{[\iota]}) - \sigma_{jl}(\tilde{z}_{j,q-o_{j,q}}^{[\iota]})\Big]\varepsilon_{l,q}\Big\}, \tag{B.3}$$

where $(\iota,k)\in(0,\aleph)_{\mathbb{Z}}\times\mathbb{Z}_0$, $i = 1, 2, \ldots, n$.

From (B.2) and (B.3), we compute

$$\|x_{i,k}^{[\iota]}\|_2 \le \Big\{\mathbf{E}\Big[e^{-\frac{1}{2}\eta_ikh}x_{i,0}^{[\iota]}\Big]^2\Big\}^{\frac{1}{2}} + \alpha_i\Big\{\mathbf{E}\Big[\sum_{q=0}^{k-1}e^{-\frac{1}{2}\eta_i(k-q-1)h}y_{i,q}^{[\iota]}\Big]^2\Big\}^{\frac{1}{2}}$$
$$\le e^{-\frac{1}{2}\eta_ikh}\|x_0\|_* + \alpha_i\sum_{q=0}^{k-1}e^{-\frac{1}{2}\eta_i(k-q-1)h}\|y_q\|_*, \tag{B.4}$$

as well as

$$\|y_{i,k}^{[\iota]}\|_2 \le e^{-\frac{1}{2}\mathscr{A}_ikh}\|y_0^{[\iota]}\|_* + \alpha_i\sum_{q=0}^{k-1}e^{-\frac{1}{2}\mathscr{A}_i(k-q-1)h}\Big[\frac{4}{\hbar^2}|\gamma_i|\|x_q\|_*$$
$$+ \hat{b}_i\|x_q\|_* + \sum_{j=1}^{n}\bar{c}_{ij}L_j^f\|x_{q-\delta_{j,q}}\|_* + \frac{1}{\sqrt{h}}\sum_{j=1}^{n}\bar{\xi}_{ij}\sum_{l=1}^{\infty}L_{jl}^{\sigma}\|x_{q-\sigma_{j,q}}\|_*\Big]$$

$$\leq e^{-\frac{1}{2}\mathscr{A}_i kh}\|y_0^{[\iota]}\|_* + \alpha_i \sum_{q=0}^{k-1} e^{-\frac{1}{2}\mathscr{A}_i(k-q-1)h}\mathscr{L}_i \max_{l\in[0,\delta_\infty]_{\mathbb{Z}}} \|x_{q-l}\|_*, \tag{B.5}$$

where $(\iota, k) \in (0, \aleph)_{\mathbb{Z}} \times \mathbb{Z}_0$, $i = 1, 2, \ldots, n$.

In view of Eqs (B.4) and (B.5), we have

$$\begin{cases} \|x_k\|_* \leq \max_{1\leq i\leq n}\left\{e^{-\frac{1}{2}\eta_i kh}F + \alpha_i \sum_{q=0}^{k-1} e^{-\frac{1}{2}\eta_i(k-q-1)h}\|y_q\|_*\right\}, \\ \|y_k\|_* \leq \max_{1\leq i\leq n}\left\{e^{-\frac{1}{2}\mathscr{A}_i kh}F + \alpha_i \sum_{q=0}^{k-1} e^{-\frac{1}{2}\mathscr{A}_i(k-q-1)h}\mathscr{L}_i \max_{l\in[0,\delta_\infty]_{\mathbb{Z}}}\|x_{q-l}\|_*\right\}. \end{cases} \tag{B.6}$$

Through condition (i_7), there exist $\varpi > 0$ and $\mathscr{U} > 0$ such that $\frac{1}{\mathscr{U}} + \max_{1\leq i\leq n}\left\{\frac{\alpha_i e^{\varpi h}}{1-e^{-(\frac{1}{2}\eta_i-\varpi)h}}, \frac{\alpha_i e^{\varpi(\delta_\infty+1)h}}{1-e^{-(\frac{1}{2}\mathscr{A}_i-\varpi)h}}\mathscr{L}_i\right\} < 1$. Next, the following fact below should be claimed: $\max\left\{\|x_k\|_*, \|y_k\|_*\right\} \leq \mathscr{U}Fe^{-\varpi kh}, \quad \forall k \in \mathbb{Z}_0$. If it is invalid, then there exists $k_0 \in \mathbb{Z}_0$ such that one of the two case below will be valid.

1) $\|x_{k_0}\|_* > \mathscr{U}Fe^{-\varpi k_0 h}$, and $\max\{\|x_k\|_*, \|y_k\|_*\} \leq \mathscr{U}Fe^{-\varpi kh}, \forall k \in [0, k_0)_{\mathbb{Z}_0}$.

2) $\|y_{k_0}\|_* > \mathscr{U}Fe^{-\varpi k_0 h}$, and $\max\{\|x_k\|_*, \|y_k\|_*\} \leq \mathscr{U}Fe^{-\varpi kh}, \forall k \in [0, k_0)_{\mathbb{Z}_0}$.

On condition that 1) holds, via (B.6), we gain

$$\begin{aligned} \|x_{k_0}\|_* &\leq \mathscr{U}Fe^{-\varpi k_0 h}\max_{1\leq i\leq n}\left\{\frac{e^{-(\frac{1}{2}\eta_i-\varpi)k_0 h}}{\mathscr{U}} + \alpha_i\sum_{q=0}^{k_0-1} e^{-\frac{1}{2}\eta_i(k_0-q-1)h}e^{-\varpi(q-k_0)h}\right\} \\ &\leq \mathscr{U}Fe^{-\varpi k_0 h}\max_{1\leq i\leq n}\left\{\frac{1}{\mathscr{U}} + \frac{\alpha_i e^{\varpi h}}{1-e^{-(\frac{1}{2}\eta_i-\varpi)h}}\right\} \leq \mathscr{U}Fe^{-\varpi k_0 h}. \end{aligned}$$

Comparing to fact 1), we have a conflict.

Similarly, when 2) is valid, inequality (B.6) induces

$$\begin{aligned} \|y_{k_0}\|_* &\leq \mathscr{U}Fe^{-\varpi k_0 h}\max_{1\leq i\leq n}\left\{\frac{e^{-(\frac{1}{2}\mathscr{A}_i-\varpi)k_0 h}}{\mathscr{U}} + \alpha_i\sum_{q=0}^{k_0-1} e^{-(\frac{1}{2}\mathscr{A}_i-\varpi)(k_0-q-1)h}e^{\varpi(\delta_\infty+1)h}\mathscr{L}_i\right\} \\ &\leq \mathscr{U}Fe^{-\varpi k_0 h}\max_{1\leq i\leq n}\left\{\frac{1}{\mathscr{U}} + \frac{\alpha_i e^{\varpi(\delta_\infty+1)h}}{1-e^{-(\frac{1}{2}\mathscr{A}_i-\varpi)h}}\mathscr{L}_i\right\} \leq \mathscr{U}Fe^{-\varpi k_0 h}. \end{aligned}$$

Likewise, this is opposed to 2). Summing up the above discussions, the claim holds. Therefore, SINN (2.1) is globally exponentially stabilized via the feedback control (4.4). The proof is complete.